LUND
UNIVERSITY

Master of Science Thesis

Manned Mission to Mars: Water as Radiation Shielding During a Solar Particle Event

Edda Lína Gunnarsdóttir

Supervisors:
Christopher Rääf, Sören Mattsson and Hannie Förnvik

Medical Radiation Physics, Malmö
Department of Translational Medicine
Lund University, Sweden
2020

Abstract

Space agencies and private companies are working hard to solve the various challenges that need to be overcome to take humans to Mars. The journey to Mars has multifaceted risks for the crew, including radiation exposure. One risk factor that could jeopardize the crew's health is the radiation dose from a large solar particle event (SPE) during Mars transit. It is therefore critically important to design a radiation shelter made of an effective shielding material. One of the shielding materials that has been suggested is water.

This thesis explores the feasibility of using water for radiation shielding during a large SPE by simulating the radiation dose to the crew in a spherical radiation shelter composed of water using NASA's On-Line Tool for the Assessment of Radiation in Space (OLTARIS) code. The amount of water needed for the astronauts not to exceed NASA's radiation dose limits was evaluated and compared to the amount of reserve water expected to be available.

The results show that using the consumption water available as shielding during an SPE reduces the radiation dose to the astronauts significantly. The results indicate that using consumption water as shielding may be sufficient to prevent the astronauts from exceeding the NASA short- and long term radiation dose limits.

Summary in Swedish

Det ligger i människans natur att utforska och söka efter det okända. Nu arbetas det hårt för att möta de stora utmaningarna som måste övervinnas för att en bemannad resa till Mars ska bli verklighet. NASA planerar att skicka människor till Mars under 2030-talet och det privata företaget SpaceX har målet att skicka en bemannad farkost till Mars så tidigt som år 2024.

Resan till Mars utgör mångfasetterade risker för besättningen, inklusive exponering av högenergetisk och komplex rymdstrålning. Strålningsmiljön i rymden skiljer sig från bakgrundsstrålning på jordytan eftersom atmosfären och jordens magnetfält stoppar och dämpar rymdstrålningen.

En riskfaktor som kan utsätta besättningen under marsresan för höga stråldoser är en så kallad solpartikelhändelse (SPE), som uppstår när solen frigör och sprider stora mängder laddade partiklar ut i solsystemet. SPE är relativt sällsynta och kan pågå från några timmar till några dagar. Lyckligtvis kan astronauter varnas innan strålningen från SPE når rymdskeppet vilket gör det möjligt för dem att söka skydd bakom en strålskärm.

Det är viktigt att utforma ett strålskydd med material som effektivt attenuerar SPE strålningen och förhindrar höga stråldoser som kan riskera astronauternas hälsa. Ett av materialen som har föreslagits är vatten eftersom det redan förvaras ombord på rymskeppet för konsumtion.

I denna studie undersöks möjligheten att använda vatten som strålskärmning under en stor SPE genom att simulera stråldosen till besättningen med hjälp av NASAs On-Line Tool for the Assessment of Radiation in Space (OLTARIS) program. Det antas att astronauterna sitter i ett ihåligt sfäriskt strålskydd som består av vatten. Mängden vatten som behövs för att stråldoserna till astronauterna inte ska överskrida NASAs dosgränser utvärderas och jämförs med mängden reservvatten som förväntas vara tillgängligt i rymdskeppet.

Resultaten visar att användning av vatten för strålskärmning under en SPE minskar stråldosen till astronauterna signifikant. Resultaten tyder på att användning av reservvatten som strålskärmning kan vara tillräckligt för att förhindra att astronauterna överskrider NASAs dosgränser.

Contents

Acknowledgments

I have had the privilege of working with three fantastic supervisors, Christopher Rääf, Sören Mattson and Hannie Förnvik, whom I thank for their valuable input, support and guidance. I also thank all the other helpful and kind people working at MSF Malmö and Lund for being welcoming and supportive.

1 Introduction

A manned mission to Mars is planned for the near future. NASA is planning on sending humans to Mars in the 2030s and SpaceX has announced the goal of sending a crew to Mars as early as in 2024. There are many obstacles that need to be overcome before manned missions to Mars are possible, both technological and biomedical. One of the biggest challenges is the radiation environment in space and its effect on the health and performance of the crew [1].

Astronauts' health is especially threatened by so called solar particle events (SPEs), sudden releases of large amounts of energetic plasma from the Sun. SPEs are relatively rare events[1] and can last from hours to days. Fortunately, the astronauts can be alerted before the radiation from the SPE reaches their spaceship in order for them to seek shelter behind a radiation shield.

An adequate SPE shield needs to meet a number of criteria. In addition to being able to effectively attenuate the SPE radiation, it should optimally serve other functions than radiation shielding alone. One material that fits these criteria is water aimed for use by the crew.

In this thesis a hypothetical scenario is explored, where astronauts utilize a spherical storm shelter composed of water during an SPE. The radiation shielding in this scenario is evaluated by simulating the radiation dose received by the astronauts using NASA's OLTARIS program.

1.1 Aims

The overall aim of this thesis is to study the feasibility of using the water supply available onboard a spacecraft as shielding during a large SPE in the transit to Mars. Specifically, the aim is to evaluate how thick a layer of water is needed in a storm shelter to ensure the crews safety[2] during a large SPE. Can such a storm shelter be constructed with the amount of reserve water available?

[1] Since 1955 there have been five SPEs large enough to constitute a health risk to astronauts.

[2] The crew is here considered safe when their estimated radiation dose is within NASA's radiation limits for acute and late health risks [2][3]. For details see chapter 2.4.2.

2 Background

2.1 Radiation Environment in Space

The radiation environment in space is a combination of radiation emanating from the Sun and high energy radiation originating from outside our solar system, called galactic cosmic radiation (GCR). The Earth's magnetic field and its atmosphere act as a radiation shield and thus protect the Earth and its inhabitants from the main hazards of the incident radiation. The radiation that penetrates this protective shield contributes to the background radiation on Earth. Some of the particles of solar- and galactic origin (as well as their secondaries) get caught in the Earth's magnetic field, creating radiation belts, consisting of protons and electrons, surrounding the planet.

Spacecrafts leaving Earth on deep space missions need to penetrate Earth's radiation belts but the radiation exposure due to this does not contribute much to the total mission exposure of the astronauts since the exit through the radiation belts only takes a few minutes [1]. When in outer space the radiation environment consists of the galactic cosmic radiation, the stream of solar particles called the solar wind and the occasional large solar proton flares called solar particle events (SPEs), as illustrated in figure 1. Here, mainly the galactic cosmic radiation and the solar particle events will be covered.

2.1.1 Galactic Cosmic Radiation

The galactic cosmic radiation (GCR) was first discovered by Victor Hess in 1912 but there is still much unknown about its origin. The GCR is an isotropic radiation of fully ionized nuclei ranging from the atomic number of hydrogen up to that of nickel. The particle composition can vary slightly but is approximately as follows: protons (hydrogen nuclei) 85%; alpha particles (helium nuclei) 14%; electrons 2% and heavier nuclei 1 % [1]. The particles that have a higher charge than alpha particles are called high charge and high energy particles (HZE).

GCR particles are accelerated into our solar system and transported by the intergalactic magnetic field. In Earth's vicinity, the particle energies range from 10 MeV to several TeV per nucleon [5]. Due to it's high energy, the GCR is thought to originate from supernova explosions or other high energy phenomena such as neutron stars or pulsars from outside our solar system [1]. The proportion of heavy ions such as iron nuclei is small compared to that of carbon and oxygen but iron nuclei are very densely ionizing and contribute substantially to the absorbed dose, which increases with the square of the particle charge [5]. This can be seen in figure 2 which shows the relative fluence, absorbed dose and dose equivalent contribution of all particle components in the GCR, respectively. For definition of radiation dose quantities see section 2.4.1.

The HZE particles of the GCR spectra travel long distances in medium before they lose all their energy. For instance, protons and iron ions with energies of 1 GeV have a range of 3.2 m and 26 cm in water and 1.5 m and 12 cm in aluminum, respectively [5]. When these heavy and energetic particles interact with matter, a spectrum of secondary radiation, including other energetic nuclei, protons and neutrons, are produced. This makes it challenging to evaluate radiation doses to astronauts in space.

A study from 2010 found the effective dose equivalent from the GCR during

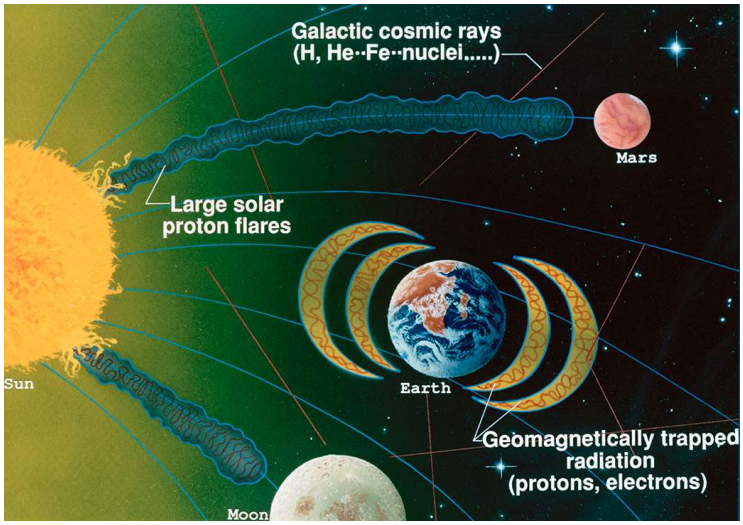

Figure 1: An illustrative representation of the radiation environment in space. Reprinted from [4].

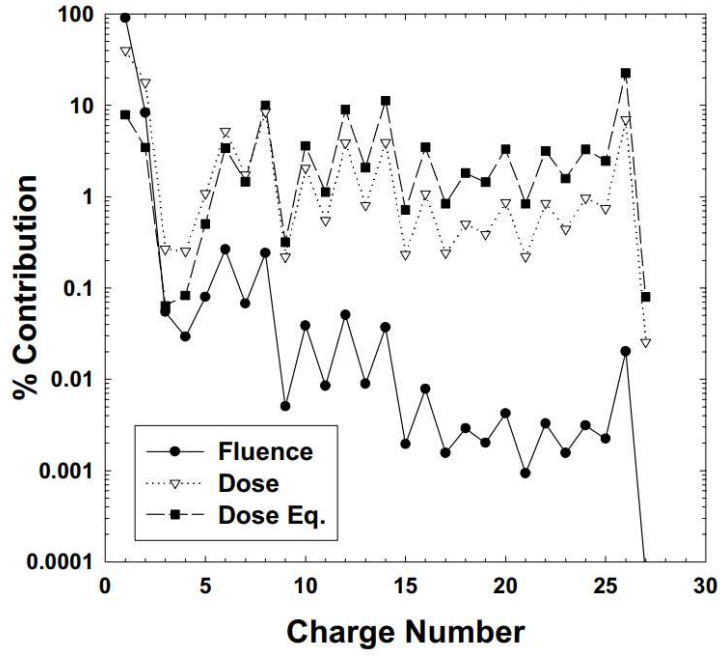

Figure 2: Relative GCR fluence, absorbed dose and equivalent dose for each element in the GCR. Notably, iron (Z=26) contributes significantly to the external dose equivalent. Reprinted from [6].

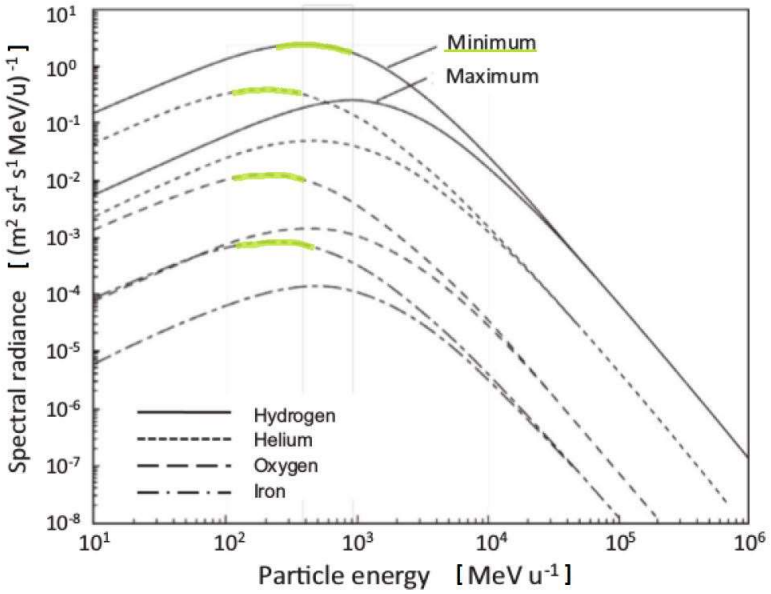

Figure 3: The energy distribution of four GCR components (H, He, O and Fe) during the 1977 solar minimum (green) and the 1959 solar maximum at 1 AU[4] from the sun, respectively. The radiance is presented as a function of the particle energies. For each element, the upper line is solar minimum and lower is maximum. Modified and reprinted from [1].

a solar minimum to be 621 mSv/y and 497 mSv/y behind 5 g/cm^2 and 20 g/cm^2 aluminum shielding, respectively [3].[3] The study showed that typical spacecraft shielding is not effective enough in attenuating the GCR. The reason for evaluating the dose at a solar minimum is that the fluence and energy of the GCR varies with the approximate 11 year solar activity cycle. There is an inverse correlation between the solar activity and the GCR fluence, resulting in a higher GCR dose during solar minimum than solar maximum. This relationship can be seen in figure 3 which shows the radiance vs. particle energy of hydrogen, helium, oxygen and iron during the 1977 solar maximum and 1959 solar minimum, respectively, at one astronomical unit from the sun (1 AU).[4] The radiance and energy of the GCR decreases during solar maximum because the particles are scattered by irregularities in the interplanetary magnetic field carried by the solar wind [2].

2.1.2 Solar Wind and Solar Particle Events

The Sun continuously emits a stream of particles that are transported throughout the solar system carrying with it the solar magnetic field. This is called the solar wind and it consists mainly of protons and electrons but also a small

[3]The effective dose equivalent values are calculated with the tissue weighting factor from ICRP 2007.

[4]The astronomical unit (AU) is commonly used in astronomy and approximately equals the mean distance between the Earth and the Sun.

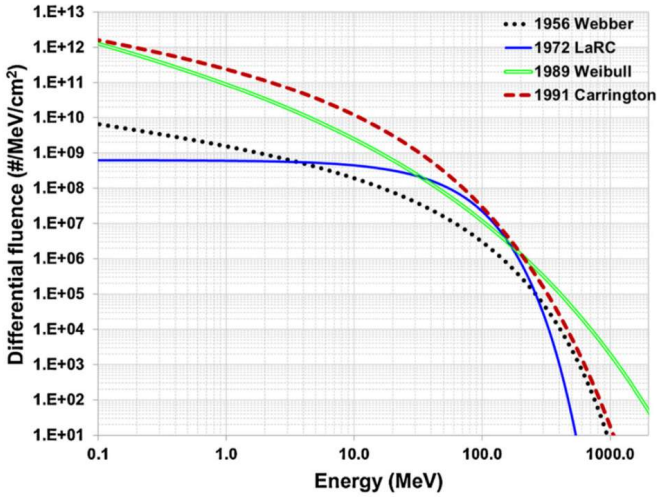

Figure 4: The differential spectra for four different historical SPE. Reprinted with permission from Elsevier [8].

fraction of He-4 ions. The solar wind particles have relatively low energies, e.g. between 100 eV and 3.5 keV for protons, and are thus very easily shielded and have no significant contribution to the radiation exposure of astronauts [1].

Occasionally, the Sun suddenly releases a large amount of energetic solar plasma. These events are called solar particles events (SPEs) and emerge as a burst of protons and electrons accelerated away from the Sun. The particles in these events have energies up to several GeV and can pose a serious threat to astronauts' health due to their radiation effects [1]. The origin of SPEs is related to solar phenomena called coronal mass ejections (CMEs) that take place in the outermost layer of the Sun, the corona. During CMEs vast amounts of energy are released in the form of electromagnetic waves, which in turn form large currents and variations in the magnetic field, causing an acceleration of solar matter into interplanetary space [1].

SPEs are stochastic events but have a higher probability of occurring around solar maxima than minima [5]. In the years between 1954 and 1994, a total of 50 SPEs with energies above 450 MeV were detected, with between 10 and 15 SPEs taking place around each of the four solar maximum in the time period [7]. Taking this into account, interplanetary travel during periods of solar maxima is unfavorable with respect to radiation from SPEs.

Although most SPE particles can be stopped by a relatively thin layer of shielding, there have been five SPEs since 1955 large enough to constitute a health risk to astronauts behind spacecraft shielding [1]. The SPE that took place in August 1972 is often described as the worst case scenario [7]. Luckily this event took place between the Apollo 16 and 17 missions. Dose simulations of the 1972 SPE have shown that the event would have caused around a 4 Sv dose to the astronauts' skin and lens behind 5 g/cm^2 of Al shielding [5].

The differential fluence spectra for the August 1972 event and three other historically large events (1956, 1989 and 1991) are shown in figure 4. The 1972 event has a soft spectrum, while the other three have harder spectra, some with

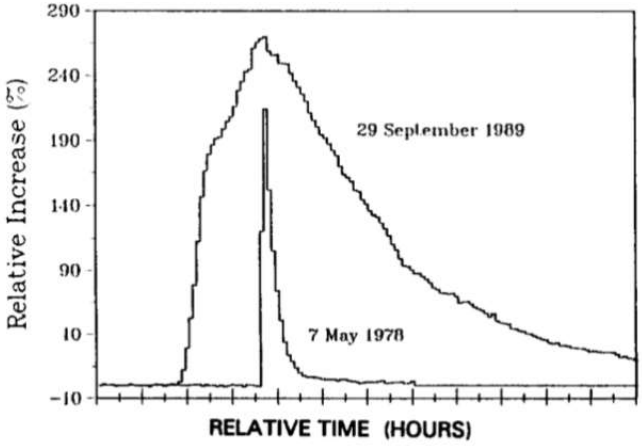

Figure 5: The duration of the largest SPE of solar cycle 22 (in 1989) compared to that of the largest of cycles 20 and 21 (in 1978). The small ticks on the time axis represents 30 minutes [7]. Reprinted with permission from Elsevier.

proton energies reaching above 1 GeV. The 1972 and 1956 SPEs have a low fluence of protons in the energy range 0-100 MeV while those of 1989 and 1991 have relatively high fluence in that energy range [8]. The event in October 1989 is comparable to the August 1972 SPE but what distinguishes the two events is the significant fluence of protons above 500 MeV in the '89 SPE [7].

Selecting a worst case SPE, in terms of dose, actually depends on several factors, such as the shielding thickness used, as demonstrated by Samy El-Jaby et al [9]. According to their study, a 2 cm thick aluminum shield results in effective dose equivalent of 0.471 Sv for the 1972 event and 0.289 Sv October 1989 event. However, for a 4 cm thick aluminum shield the October 1989 effective dose equivalent of 0.202 Sv exceeds the 1972 dose of 0.160 Sv. Additionally, for thicknesses 6, 8 and 10 cm aluminum, the effective dose equivalent in the October 1989 event exceeded that of the 1972 event. For this reason, the October 1989 event is selected as a representative worst case event in this thesis.

Another approach of selecting a worst case SPE, in terms of dose, is to consider not only the radiation dose from a single historically large SPE but rather to look at the historically large cumulative dose from all SPEs occuring over a 30 day or 1 year time interval. This was done by Samy El-Jaby et al, who showed that the cumulative SPE dose over time results in higher SPE dose estimates than looking at single events [9].

SPEs vary greatly in composition, flux and duration [7]. The SPEs can last from hours to days. Figure 5 shows the duration of the largest SPE of solar cycle 22 (in 1989) compared to the the largest of cycles 20 and 21. Although SPE radiation is emitted directionally away from the sun, it becomes isotropic further out (such as at a point between Earth and Mars) in the middle and late phases of the SPE [10].

Travelling into deep space during a solar maximum has the advantage of a relatively low GCR dose but a higher probability for one or more SPE to occur and vice versa. Since it is possible to shield against the SPE but very difficult

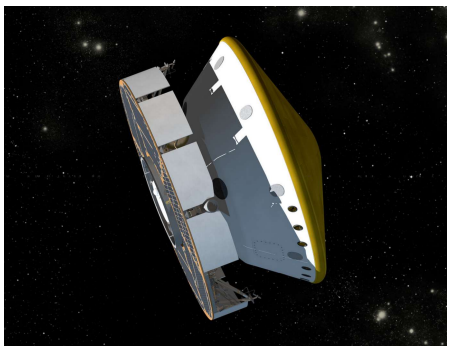

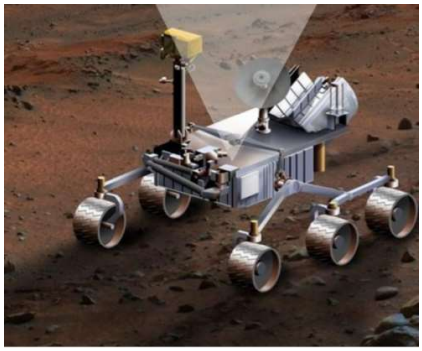

Figure 6: Artist's representation of the MSL spacecraft encompassing the Curiosity rover during the cruise phase (left image) [14]. An old design of the Curiosity rover showing RAD's position on the deck (right image). The cone shows the instrument's charged particle field of view [15]. Reprinted from [14] and [15].

to reduce the dose from GCR, it is favourable to travel to Mars during a solar maximum, given sufficient SPE shielding [2]. This shielding could be in the form of a storm shelter, taking into account the locally isotropic radiation of the SPEs.

2.2 Radiation Detection in Mars Missions

The Radiation Assessment Detector (RAD) investigation is an ongoing study of the radiation environment on Mars and during Earth-Mars transit. The RAD is a part of the Mars Science Laboratory Mission (MSL) which was designed by NASA with the purpose of studying the habitability of Mars [11]. The MSL launched in November 2011 and after a successful eight months cruise from Earth, the MSL landed on Mars on August 6th 2012, encompassing the MSL Curiosity rover [12]. The rover contains the radiation assessment detector along with ten other science instruments that have been used to study the Martian environment since its arrival.[5] Figure 6 shows, on the left, the configuration of the MSL spacecraft during the cruise phase to Mars and on the right an older design of the Curiosity rover showing RAD's position on Curiosity's deck and the the instrument's 65 degree field of view for charged particle detection.

The primary scientific objective of the RAD investigation is to measure the energetic particle spectra on Mars. Other objectives include measuring the dose at the Martian surface and determining dose equivalent rates for upcoming human missions. The scientific community will use these measurements for the validation of transmission models and radiation transport codes [16, p. 505].

The RAD has performed the first direct radiation measurements on the surface of Mars but measurements were not only performed upon arrival on Mars but also during the cruise [16]. These are the first ever measurements of the radiation environment inside a spacecraft travelling from Earth to Mars [17]. The transit measurements (which detected the GCR, SPE and their secondary

[5]The other instruments are three cameras, four spectrometers, a neutron detector, an environmental sensor and an atmospheric sensor [13]

radiation) provide valuable information on the potential radiation hazard for human missions to Mars.

RAD operated and performed measurements inside the MSL spacecraft for seven months on its journey to Mars [17]. During that time, a total of five SPEs were detected with an integrated dose equivalent of 24.7 mSv, which is comparable to 15 days of GCR exposure inside a spacecraft, at low solar activity [18]. The SPEs observed by RAD were much less intense than historically large SPEs.

The dose equivalent rate from GCR during the cruise was 1.84 $\pm$0.30 mSv/day [12]. Given the NASA design reference mission of a 360 day round trip to Mars, the total mission dose equivalent for the cruise would be 662$\pm$108 mSv [12]. The resulting dose is strongly dependent on the shielding used and the solar activity at the time of travel.

The particle spectra, dose and dose rate results from the transit to Mars are described in detail by Zetlin et al. [18], Hassler et al. [12], Guo et al. [17], Guo et al. [19], Köhler et al. [20] and Ehresmann et al. [21]. In the following section, the main properties of the radiation assessment detector are summarized.

2.2.1 The Radiation Assessment Detector

The RAD was specifically designed to measure charged particle spectra, measure the absorbed dose and determine the dose equivalent rate at the surface of Mars [12, p. 15]. The RAD can detect charged particles, neutrons and gamma radiation and has a wide dynamic range to accommodate with the large energy interval of the incoming charged particles [16].

The detector consists of the RAD Sensor Head and the RAD Electronic Box but the latter is not discussed further here. Figure 7 shows RAD before it was installed onto the Curiosity rover (left) and a cross section of the instrument (right).

A solid-state detector forms the telescope of the instrument, consisting of three silicon pin diodes that are used for the detection of charged particles (A, B and C in figure 8) [17, 16]. Detectors A and B define, in coincidence, the acceptance angle. Detector A is at the top of the detector and is in plane with the rover's deck, demonstrated in figure 6. The detection of neutrons and gamma particles is carried out by a thallium doped Cesium Iodide (CsI(Tl)) scintillator and a plastic scintillator (D and E in figure 8) [17]. The CsI(Tl) scintillator also stops charged particles with up to moderate energies. A second plastic scintillator is used for anticoincidence, i.e. for the rejection of charged particles entering from the sides and bottom of the instrument [16].

The radiation assessment detector is able to measure all ion species on Mars. It can obtain the differential flux for moderate energies and integral flux for higher ones. The ion species with moderate energies can be identified because for these particles, the energy loss per unit distance (dE/dx) and the total energy of the particle can be determined. Figure 9 shows the energy range detected for each particle type [16]. Charged particles that stop and deposit all their energy in the detector are called stopping particles and are referred to as fully analysed particles in figure 9. The energy distribution of these particles can be reconstructed because their total energy, charge and mass can be determined [17]. Charged particles that leave the detector without depositing all their energy, on the other hand, are called penetrating particles (partially analysed

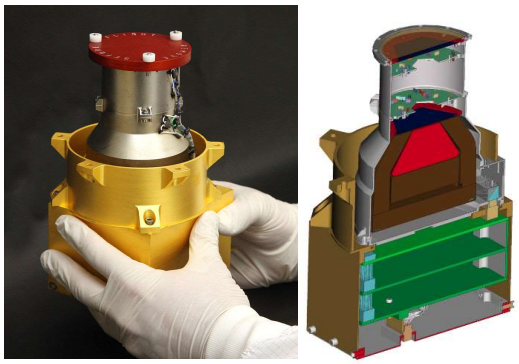

Figure 7: The Radiation Assessment Detector (RAD) before installation onto the Curiosity rover (left). A cross section of the RAD Sensor Head and the RAD Electronic box (right), image credit: NASA/JPL-Caltech/SwRI [22].

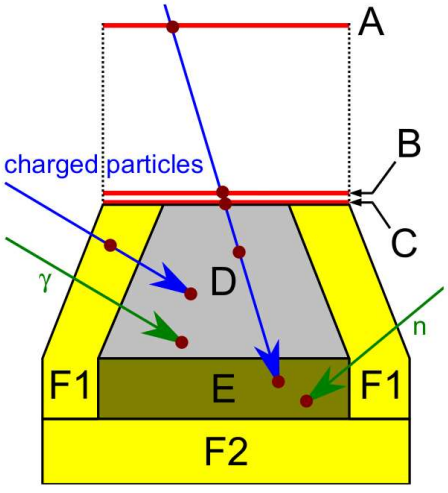

Figure 8: Schematic diagram of the RAD sensor head consisting of three silicon detectors (A,B and C) forming the telescope, a thallium doped Cesium Iodiode scintillator (D), and two plastic scintillators (E, F1 and F2) [17]. By permission of Oxford University Press.

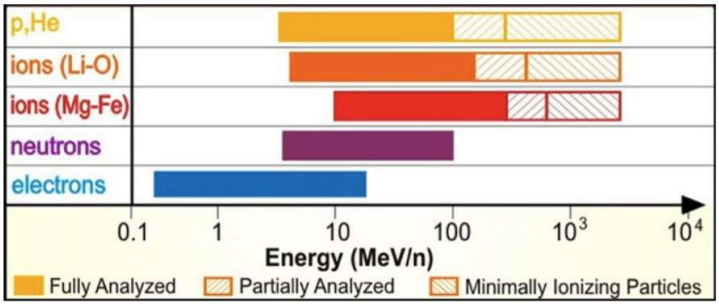

Figure 9: The ion species and ion groups that the RAD is able to identify with the corresponding energy interval measured [16]. Reprinted by permission from Springer Nature.

particles in figure 9). For these particles, only the charge and the dE/dx can be determined [16]. Both the CsI(Tl) and the plastic scintillator are sensitive to gamma radiation and neutrons but the former is an efficient gamma detector and the latter is a good neutron detector but not very good for gamma detection [16]. Although uncharged, neutrons are also referred to as fully analysed particles by RAD, according to the above description. For details on the particle detection see Hassler et al. [16].

When looking at the RAD transit measurement results it is important to be aware of the shielding distribution around the detector. The shielding above the RAD field of view (FOV) in the MSL spacecraft during the cruise phase is complex due to its positioning inside the spacecraft. The shielding thicknesses of the RAD FOV ranges from 1 up to around 80 g/cm^2 in aluminum-equivalent values but a large part of the detector solid angle is lightly shielded with 1-3 g/cm^2 [21]. The average shielding thickness of the total FOV, during the cruise phase, is about 27.5 g/cm^2 but the average shielding below the instrument is about 5 g/cm^2 [21]. The shielding of the future space vehicle carrying astronauts to Mars will most likely differ from this by being more uniform and without lightly shielded areas around the habitat [18].

2.3 Transport codes

Radiation transport calculations are essential for the estimation of the radiation field inside spacecrafts and the subsequent radiation exposure of astronauts on space missions. These calculations are performed by transport codes that use models of the radiation field in free space as a starting point and calculate the interaction of primary and secondary radiation with walls and equipment to find the radiation field inside the spacecraft. The resulting radiation field can then be used to calculate the astronaut exposures using a computational anthropomorphic phantom.

There are two types of transport codes: stochastic Monte Carlo codes and deterministic codes. The stochastic Monte Carlo codes simulate, using statistical models and random sample generator, the interaction of individual primary particles in the incoming radiation field or the secondary particles, produced by interactions of primary particles, with matter. It generate histories of

charged particles transference and energy deposition in the material. Deterministic transport codes calculate the transit of charged particles through matter by using analytical methods and approximations to solve the Boltzmann transport equations for atomic and nuclear collision [1, p.98].

2.3.1 OLTARIS

The On-Line Tool for Assessment of Radiation (OLTARIS) is a web-based radiation analysis tool specially designed for simulating space radiation environments using an analytical code. OLTARIS is fast but cannot treat 3-D radiation fields like the Monte Carlo codes LUKA, GEANT and MCNPX that enable more realistic geometries and more accurate results [16, 8]. In addition to having a short computation time, compared to other transport codes, OLTARIS has the advantage of being accessible, having a gentle learning curve and a user-friendly interface. The predefined radiation environment, geometries and phantoms, along with these properties, make OLTARIS a favorable choice for this study.

For calculations of particle transport, OLTARIS uses the deterministic code HZETRN2005 (High Z and Energy TRaNsport) which is developed by NASA Langley Research Center. The transport of charged particles is modeled by solving the Boltzman equation using the continuously slowing down approximation (CSDA) and the straight ahead approximation, which assumes that secondary particles travel in the same direction as their primaries. By making these approximations, the Boltzman equation has only one spatial dimension and no angular dimension which simplifies the computation [23]. OLTARIS uses a predefined spectral flux/fluence of the radiation environment and then transports the radiation through a slab or thickness distribution chosen by the user. A response function is applied on the transported radiation to compute the response requested by the user, for instance the point dose, the organ dose, the whole body effective dose equivalent or the output spectra [23].

Figure 10 shows a screenshot of a part of the OLTARIS user interface where a new project is being created. There are various predefined radiation environments in OLTARIS, including different models of the GCR (the most recently added being the Badhwar-O'Neil 2014 GCR model) and numerous historical SPE spectra, represented by differential formulas, available. The user can also model a new SPE spectra. For both the GCR and SPE models, the radiation environment can be selected, e.g. free space at 1 AU, Lunar surface or Martian surface.

For the calculation of effective dose or organ dose, there are four human body models available in OLTARIS: the Male Adult Voxel (MAX), the Female Adult Voxel (FAX), the Computerized Anatomical Male (CAM) and the Computerized Anatomical Female (CAF). The MAX and FAX are more accurate than CAM and CAF and the MAX-model was used in this thesis [24]. Since 2005, the MAX is based on segmented images of a male and its anatomical properties are based on the ICRP 89 (2002) reference adult male [25].

In OLTARIS, the effective dose equivalent can be calculated with the ICRP 60 quality factors and weighting factors, respectively. Another option is to use NASA quality factors and NASA tissue weighting factors (for either average US population or average never-smoker population).

The organ doses can be obtained as the average dose equivalent using either ICRP 60 or NASA quality factors, respectively, or in terms of a quantity called

gray-equivalent, which is calculated with the relative biological effectiveness (RBE) factors from NCRP report no. 132 [26, 27].

The non-biological uncertainty reported in the OLTARIS documentation for integrated dose quantities, e.g. the dose equivalent, is around 25% for crew exploration vehicle and lunar missions and a factor of two for the Martian surface [28]. The uncertainty in the dose quantities evaluated in this thesis are thus expected to be in that range. The main factors contributing to this uncertainty are the external radiation environment models, the transport algorithm and the nuclear and atomic physics models.

Simulation results from OLTARIS have been compared with results from other transportation codes in several publications. Agahara et. al. compared the dose equivalent from four SPEs using the Monte Carlo codes PHITS and MCNPX, as well as OLTARIS. They found that MCNPX and PHITS agreed better as compared to OLTARIS and that the mean relative difference of the dose equivalent between OLTARIS and the other codes was from -22.4% to +27.6% [8]. A study by Samy El Jaby et. al. found that for the SPE in October 1989, the OLTARIS dose results were 25% larger than the MCNPX results for a 2 cm aluminum shielding and 80% larger for a 10 cm shielding [9].

2.4 Radiation Protection Quantities

As described in section 2.1, the radiation field inside a spacecraft travelling in deep space consists of high energy charged particles, ranging from protons up to heavy nuclei such as iron. Additionally, the interaction of the primary field with the space vehicle produces secondary radiation in the form of photons, electrons, neutrons and other reaction products. This radiation environment differs significantly from the exposure situations on Earth that conventional radiological protection quantities have mainly been designed for. In space, the dose rates and doses are higher and the range of particle types and energies are broader than on Earth [1]. For this reason, some radiological protection quantities used on Earth are not suitable in space and new quantities should be considered.

According to ICRP publication 123, it is not appropriate to apply the ICRP 103 radiation weighting factor w_R=20 for all heavy ions in space because of the significant contribution of heavy ions to the total dose. For a more realistic risk estimate, the quality factor should be used instead, either as a function of the linear energy transfer (LET) or the particle charge and energy [1].

Radiation exposure in space leads to higher doses than are generally seen on Earth and therefore deterministic effects need to be thoroughly addressed. In space, where the radiation field can constitute high LET radiation and the radiation doses can reach the level of which deterministic effects can occur, the ICRP (in publication 123) recommends the use of RBE weighted mean absorbed dose in an organ or tissue for the risk estimation of deterministic effects [1, p. 73]. In NCRP Report no. 132 it is argued that the organ dose equivalent should not be used for deterministic effects since it is based on the quality factor which is only applicable to stochastic effects [27].

The study of space radiation and the corresponding health risks involve large uncertainties. The lack of human epidemiology data and lack of knowledge on the radiobiology of heavy ions introduce large uncertainties, along with the

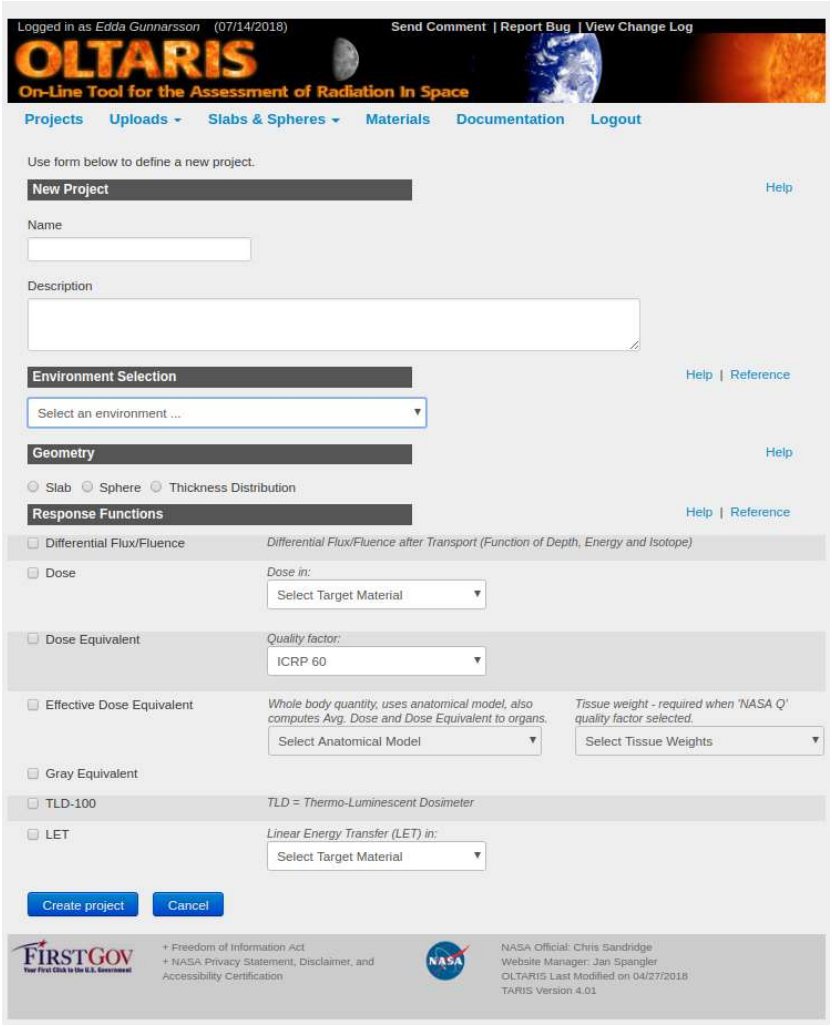

Figure 10: A screen-shot of the OLTARIS user interface where the user defines a new project [29].

radiobiological effect of dose rate and the extended radiation exposures in space [3].

2.4.1 Dose Quantities

The radiation exposure limits at NASA for the risk of fatal cancer are specified in the quantity effective dose by an age and gender specific risk factor and for the short term and non-cancer risks (deterministic effects) in gray-equivalent [2, 3, p. 117]. Although termed 'effective dose' in the publications by Cucinotta et al., this is not the effective dose defined by ICRP in report 103, but resembles more the effective dose equivalent defined in ICRP report 123, in that they both use a quality factor as the quantity for the biological effectiveness of the radiation rather than radiation weighting factor [1, 30]. The difference between these two quantities lies in the risk factor used for the biological effectiveness of different types of radiation. For clarification, the most commonly used radiological quantities in space and on Earth are presented here. The definitions and notations are mostly based on definitions in ICRP Publication 123 [1].

Dose equivalent in tissue (or an organ), $H_{T,Q}$**,** is the mean absorbed dose, D_T, times the the mean quality factor, Q_T, in tissue, T:

$$H_{\mathrm{T,Q}} = D_{\mathrm{T}} Q_{\mathrm{T}} \ . \tag{1}$$

The SI unit of dose equivalent in tissue is sievert (Sv) with the base units J/kg. This is an operational quantity (defined by ICRU) rather than a protection quantity. Originally defined in ICRP Publication 26 but then replaced by 'equivalent dose in an organ or tissue' in Publication 60 [1].

Quality factor, Q**,** reflects the biological effectiveness of radiation based on the relative difference in the LET between high- and low-LET radiation. It is conventionally given by a function of the unrestricted LET in water, L, and is defined at a point in tissue by

$$Q = \frac{1}{D} \int_{L=0}^{\infty} Q(L) D_L \mathrm{d}L \ , \tag{2}$$

where at that point, D is the absorbed dose and D_L is the distribution of D in unrestricted linear energy transfer. The distribution of D_L is integrated over the total LET spectrum. The relationship between the Q-value and the LET, defined by ICRP Publication 60, is [30, p. 30]:

$$Q(L) = \begin{cases} 1 & L < 10 \text{ keV}/\mu\text{m} \\ 0.32L - 2.2 & 10 \leq L \leq 100 \text{ keV}/\mu\text{m} \\ 300/\sqrt{L} & L > 100 \text{ keV}/\mu\text{m} \ . \end{cases} \tag{3}$$

The quality factor is used for estimating cancer risk and is preferred for risk estimations in space radiation over the radiation weighting factor, described below [2, p. 5].

The definition above is the conventional definition of the quality factor. NASA has developed a new method where the quality factor is based on the energy and charge of the particles and allows for a more precise uncertainty assessment to be made than using the conventional quality factor [2, p. 122].

This way the large uncertainty in the radiobiology of heavy and energetic particles is taken into account [18]. More on the NASA quality factor is found in section 5.6 in *Space radiation cancer risk projections and uncertainties-2012* [2]. The NASA quality factor is used in this thesis since resulting dose values are compared with NASA permissible exposure limits.

Effective dose equivalent, H_E, is the product of the dose equivalent in tissue, $H_{T,Q}$, and the tissue weighting factor, w_T, summed for all specified tissues of the body:

$$H_{\mathrm{E}} = \sum_{\mathrm{T}} w_{\mathrm{T}} H_{\mathrm{T,Q}} \ . \tag{4}$$

The SI unit of effective dose equivalent is sievert (Sv). Originally defined in Publication 26 but then replaced by the 'effective dose' in Publication 60. This quantity, when used with NASA's Q-factors and NASA's gender specific tissue weighting factors, is called effective dose at NASA, but should be called NASA Effective Dose when used externally [2, p. 122]. The results in this thesis are presented in terms of NASA's Effective Dose, called effective dose equivalent in the text.

Tissue weighting factor, w_T, represents the relative contribution of that tissue (or organ) to the overall radiation risk from stochastic effects when the whole body is irradiated uniformly. It is defined such that the sum of all tissue weighting factors of the body is one. The factor does not depend on the radiation quality [31]. ICRP tissue weighting factors are specified in the most recent ICRP publication 103 and in the older ICRP publication 60. More recent tissue weighting estimates have been performed by NASA, called NASA tissue weighting factors. They are gender specific, for adults at typical astronaut ages (30 to 60 y) and are based on models for the average U.S. population and a never-smokers U.S. population [32, p. 122-123]. For an overview of ICRP and NASA tissue weights, see table 6.3 in see reference [32, p. 123].

Gray-equivalent, G_T, is a quantity, and not a unit in this case, defined as the dose that is weighted for relative biological effectiveness. It is the mean absorbed dose in an organ or tissue, D_T, times the relative biological effectiveness, RBE, of the particle type i:

$$G_T = RBE_i D_T \ . \tag{5}$$

The SI unit of D_T is gray (Gy) and the quantity is notated as Gy-Eq [27, 31]. NASA uses this quantity for short term and non cancer dose limits in space.

Relative Biological Effectiveness, RBE, is the ratio of the absorbed dose of a reference radiation to the absorbed dose of the radiation considered needed to give identical biological effect. This quantity is recommended for use in estimating the risk of deterministic effects in space [2, p. 5][1, p. 73]. The RBE is determined experimentally. The values vary with absorbed dose, absorbed dose rate, and the particular biological endpoint studied. The RBE value for protons with energies larger than 2 MeV is 1.5 for skin risks with the end-point being clinically significant skin damage and for the blood forming organ risk with in-flight sickness or death being the end-point [3]. For the RBE values of other particle types see table 1.2. in NCRP report no. 132 [27].

Equivalent dose in tissue (or an organ), H_{T}, is the mean absorbed dose, $D_{\mathrm{T,R}}$, from radiation of type R in the specified tissue, T, multiplied by the radiation weighting factor, w_{R} and summed over all radiation types:

$$H_{\mathrm{T}} = \sum_{\mathrm{R}} w_{\mathrm{R}} D_{\mathrm{T,R}} \ . \tag{6}$$

The SI unit for equivalent dose is sievert (Sv). The quantity is not used in space dosimetry because the radiation factor is not applicable in the space radiation environment [1, p. 145]. Consequently, the same is valid for the effective dose, described below.

Radiation weighting factor, w_R**,** is a dimensionless factor that accounts for the difference in the biological effectiveness of high-LET radiation compared with low-LET radiation. It is applicable for estimating stochastic effects and is used in the calculation of the equivalent dose, H_T. The radiation weighting factor is assigned based on particle type and is independent of the tissue or organ irradiated [31, p. 18, 124]. Due to the strong contribution of heavy ions in the radiation field in space, the weighting of radiation is based on the radiation quality factor, Q, (which is a function the particle LET) instead of the radiation weighting factor, w_R. The application of w_R is restricted to low dose rates and low doses and is thus not appropriate for dosimetry in space [1, p. 63,145]. The most recent numerical values of w_R are defined in ICRP publication 103 [30].

Effective dose, E**,** is the product of the equivalent dose in the specified tissue (or organ), H_{T}, and the corresponding tissue weighting factor, w_T. The product is summed over all specified organs and tissues of the body:

$$E = \sum_{\mathrm{T}} w_{\mathrm{T}} H_{\mathrm{T}} \ . \tag{7}$$

The SI unit for effective dose is sievert (Sv). The quantity is not applicable in space dosimetry due to the radiation weighting factor, w_R in the equivalent dose in tissue [1, p. 145].

2.4.2 Radiation Dose Limits for Space Missions

Astronauts are not classified by ICRP as being occupationally exposed in the same way as radiation workers on Earth and aircraft crew are. Their exposure to ionizing radiation from natural radiation sources is considered a special case of environmental exposure and ICRP defines it as an existing exposure situation. In the exceptional radiation environment outside the Earth's magnetosphere, the radiation exposure of astronauts on exploration missions will exceed the radiation limits recommended for occupational exposure on Earth in ICRP Publication 103. According to ICRP, each space mission can be evaluated separately with respect to reference levels, so appropriate reference levels for risks and doses may be selected and there is even an option to not apply any dose limits for a specific mission [1, p. 29-30].

The National Council on Radiation Protection and Measurements (NCRP) has recommended special dose limits for astronauts in low Earth orbit (LEO) in NCRP Reports No. 132 and 142 [27, 31]. The NASA radiation limits are based

Table 1: The NASA permissible exposure career limits for a 1 year mission based on the average US adult population. Data is originally from Cucinotta et al. [2, p. 117].

Age	**Females [Sv] (never smoker)**	**Males [Sv] (never smoker)**
30	0.44 (0.60)	0.63 (0.78)
40	0.48 (0.70)	0.70 (0.88)
50	0.54 (0.82)	0.77 (1.00)
60	0.64 (0.98)	0.90 (1.17)

on these reports but the NASA radiation protection program defines new dose limits for astronauts on exploration missions [2].

Dose limits are designated for stochastic and nonstochastic biological effects of radiation. The nonstochastic effects (deterministic effects) are early or late effects resulting from high dose exposure that causes a significant fraction of cell loss leading to the malfunction of tissue [3]. The deterministic effects emerge above a certain threshold dose while the stochastic effects are late effects that can result from low radiation doses and seem to have no threshold. Low doses can cause changes in a small number of cells leading to an increased risk of cancer. Other possible late biological effects involve damage to the central nervous system and heart disease risks [3].

The principle of as low as reasonably achievable (ALARA) ensures that radiation limits as described here should not be treated as tolerance values. Measures should be taken to ensure that radiation doses do not approach the dose limits [33]. Every space mission should also include a detailed cost versus benefit analyses of different methods to improve the radiation safety of the astronauts [3].

The NASA permissible exposure limits for exploration missions restrict astronaut exposure to a 3% risk of exposure-induced death (REID) from cancer with an additional requirement to use the upper 95% confidence level in the risk projection model [2, p. 1]. The REID takes into account cancer deaths that take place at an earlier age due to radiation exposure. Table 1 presents these limits in terms of effective dose equivalent (also called the NASA effective dose) for a 1 year mission or less. For definitions of dose quantities see section 2.4.1. An equal organ dose equivalent, $H_{T,Q}$, for all organs is assumed (ideal case of uniform whole body irradiation) and for the application of these limits, the crew should have no prior occupational radiation exposure. Limits are presented for males and females assuming the average United State Adult and someone who has never smoked, respectively. The table shows that the REID is higher (and thus the dose limits lower) for women due to the difference in tissue types and sensitivities between sexes and because women have a longer life expectancy. The dose limits increase with age for both sexes because of the shorter time interval possible to develop a radiation induced malignancy. The lifetime risks for a fatal heart and CNS disease are included in these limits. For other mission durations than the 1 year time duration assumed in table 1, new limits can be calculated [33, p. 75-76].

The short term or non-cancer dose limits are presented in table 2 for critical organs in terms of gray-equivalent (section 2.4.1). The table includes the 30 day

Table 2: The NASA short term or non-cancer exposure limits [3].

Organ	**30 day Limit [mGy-Eq]**	**1 year Limit [mGy-Eq]**
Lens	1000	2000
Skin	1500	3000
BFO	250	500
Heart	250	500
CNS	500	1000

and 1 year limits but only the former is applied in this thesis. For the original table with career limits included as well see Cucinotta et al. [3].

The purpose of these dose limits for short term or non-cancer effects is twofold: Preventing in-flight risks that could endanger the mission success and prevent or limit the risk of degenerative tissue diseases occurring at later times. The relative biological effectiveness factors used to obtain the radiation dose limits in terms of gray-equivalent in table 2 are related to the following biological effects, also called end-points.

The dose limit for the blood forming organs are set with respect to end-points such as nausea, vomiting, and fatigue. The limits set for the lens, skin, heart and CNS restrict the risks of degenerative tissue diseases appearing as late effects. These are for example cataract, stroke, coronary heart disease or dementia [3]. The end-points related to the RBE used for setting gray-equivalent limits for skin and lens are clinically significant lesions that have been determined with fractionated doses [27]. Also, the lens limits should prevent early severe cataracts.

The limits for CNS and heart disease risk are relatively new limits and are based on NASA assessment of human studies and radiobiology. These limits are expected to be rather uncertain due to the limited radiobiological data on non-cancer effects [3].

2.5 Radiation Shielding

New challenges emerge when designing radiation shielding for travelling beyond the Earth's magnetosphere and its shielding against the GCR and SPEs. The mitigation of the low but constant rate of GCR exposure with shielding is difficult because of the high energy particles and the secondary particles produced in the shielding material. An unfeasibly large layer of shielding material is necessary for effective shielding against GCR, which makes this an ongoing research topic where innovative solutions are needed [34]. Indirect GCR shielding approaches might be necessary, for example by limiting the time duration of the transit and travelling at solar maximum when the GCR exposure is minimized. The SPE exposure, in contrast to the GCR, can be effectively reduced because it involves primarily low and medium energy protons that are effectively stopped with hydrogen rich shielding materials. Large SPEs are rare and short lived but they come with high exposure rates. With a radiation warning system and a sheltered area for the crew during high exposure periods, the SPE risk can be effectively reduced [34]. Figure 11 demonstrates the difference in shielding effectiveness of aluminum for GCR and SPE exposures, respectively. The figure shows the integral LET distribution of effective dose behind 5, 10 and 20 g/cm^2

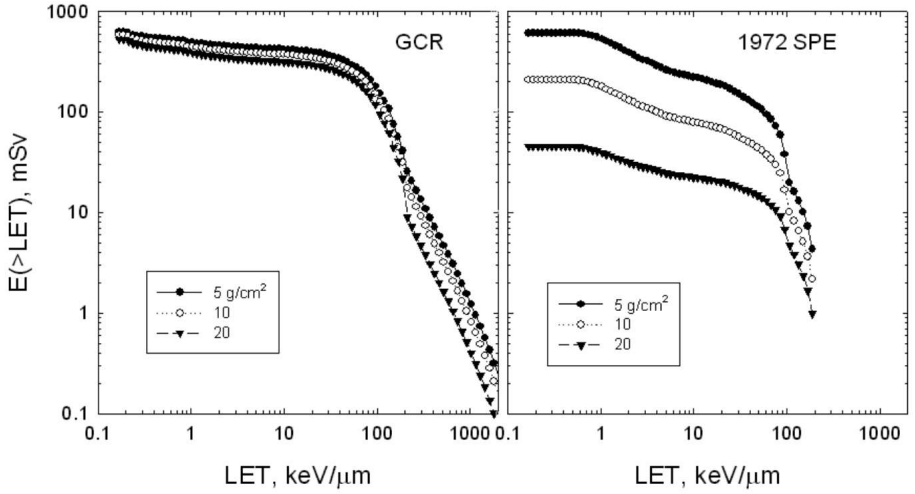

Figure 11: The integral LET distribution of effective dose shows the shielding effectiveness of 5, 10 and 20 g/cm^2 aluminum from annual GCR exposure at solar mininum and the 1972 SPE. Reprinted from [3].

aluminum shielding for annual GCR at solar minimum and the 1972 SPE [3]. These effective dose predictions were performed with the HZETRN code by Cucinotta et al. [3] and show how challenging it is to reduce the radiation risk from GCR exposure with shielding compared to the SPE exposure.

Materials used for radiation shielding in space should optimally be multifunctional, lightweight and withstand mechanical loading and extreme temperatures [35]. The materials should preferably work as building blocks for the spacecraft (or perform some other necessary functionality - in addition to radiation shielding) to minimize the launch cost, which is strongly dependent on the mass that needs to be launced into space. Materials with high charge-to-mass ratio provide the most efficient shield for both SPE and GCR [36]. Hydrogen is therefore a favorable element to be included in the shielding material because of its effectiveness in fragmenting the HZE particles in the GCR, stopping protons in the SPE and slowing secondary neutrons produced by interaction processes of GCR and SPE with other shielding material. However, hydrogen rich material such as polyethylene does not typically have the strength or stability to be a structural element of a spacecraft [35]. Aluminum, compensated with nonstructural polyethylene or water, has instead been the standard for radiation shielding and building blocks in spacecrafts carrying humans to space [36, 35]. Typical shielding thicknesses for a space suit, the spacecraft and a special radiation shielding area in the spacecraft are 0.3, 10 and 30 g/cm^2 aluminum, respectively [37].

According to a NASA study from 2012 [36] the development of new multifunctional shielding materials with high hydrogen content that reduce the risk from space radiation should be encouraged. Ongoing research into nanomaterials for radiation shielding in space shows promise in this area as reported by Thibeault et al. [35]. Figure 12 demonstrates the shielding effect of a series of shielding materials for the 1972 SPE, where the dose equivlent is presented

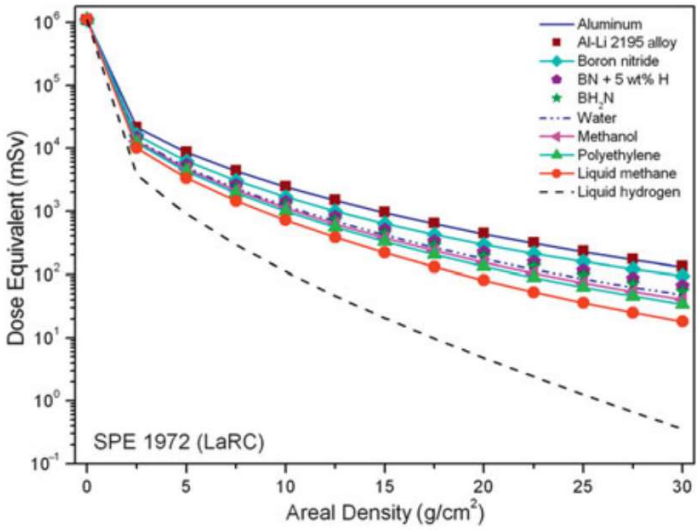

Figure 12: Shielding effectiveness of various materials for the 1972 SPE presented as a function of the areal density [38][35]. Reproduced with permission.

as a function of the areal density [35]. These predictions were made using the OLTARIS transport code. The materials shown in figure 12 include boron nitride (BT) with varying weight percentages of hydrogen, because hydrogenated boron nitride nanotubes (BNNTs) might be used for structural application and is a promising candidate [35]. Figure 12 shows that the shielding effectiveness increases with the hydrogen content of the shielding material with liquid hydrogen being the most efficient shielding agent. Water has good properties for shielding but comes with the downside of being a liquid at operating temperatures and not a structural material [35]. It is still necessary to have water on space exploration missions so it would be beneficial to also utilize its radiation shielding properties.

2.5.1 Water Supply

One reason for studying water for shielding is that it is inevitable to have water onboard the spacecraft for eating, drinking and general hygiene. It is not clear how much water will be available for the crew on exploration missions since it depends on what water supply method will be used. The options are, according to Jones et al. [39], either to use fuel cell and storage water, which has been the choice for short missions including Apollo and the transits to the International Space Station (ISS), or recycling the water with an efficient life support system, as is done on the ISS. Regardless, there will have to be a certain amount of reserve water onboard the spacecraft. An analysis of the water consumption of the crew on the ISS showed that the water requirement for each crew members is 5.32 kg (or litres) of water per day [39]. This can be applied to future Mars missions and with a crew of four, the daily water requirement would be 21.28 kg. The ISS analysis excluded dish washing and most of the crew hygiene water, it thus represents the minimum amount of water per person per day [39]. Also,

if the food is completely dehydrated, there is a need for additional 1.15 kg water per astronaut per day but potentially that water will be stored in the food [39]. On the other hand, the maximum hypothetical amount of water available to the crew travelling to Mars, in the extreme and unrealistic case, is the max payload of the spacecraft. The Falcon Heavy, a Space X rocket that is the most powerful operational rocket in the world, will have a max payload of 16.8 tonnes when flying to Mars [40]. The retired NASA space shuttles (Columbia, Challenger, Discovery, etc.) that have gone on numerous LEO missions, encompassed a 300 litre water tank and ongoing projects aim to use these tanks again for future reserve water on ISS with a total capacity of 600 litres [41, 42]. The amount of reserve water in future Mars missions will depend on factors such as the properties and quality of the water supply system. In this thesis, three days of reserve water was assumed to be available for shielding purposes.

3 Materials and Methods

3.1 Experimental Setup

To evaluate the amount of water needed to protect the astronauts from exceeding the NASA radiation dose limits during a historically large solar particle event, this thesis studies one specific mission scenario. In this hypothetical mission, four astronauts are travelling to Mars and a 180 day transit time is assumed, in accordance with one of the suggested NASA reference missions [43]. For simplicity, the spacecraft design is such that it has an external radiation storm shelter (see figure 13). The distance from the main compartment to the radiation shelter is made large such that the main compartment does not have any shielding effect and only the material of the storm shelter provides radiation shielding. This spacecraft geometry is convenient for the modeling of the dose to the astronauts and makes it possible to evaluate the shielding effect of the storm shelter only.

The radiation storm shelter is assumed to be a hollow sphere with walls made of the reserve water available onboard the spacecraft. The astronauts reside in the main compartment of the spacecraft during the transit, except when large solar particle events occur, during which the astronauts seek protection in the radiation storm shelter. Figure 14 shows how the astronauts are assumed to sit compactly in the storm shelter, surrounded by a hollow water sphere.[6] The inner diameter of the sphere is assumed to be 1.5 meters and the entry/exit is assumed to be of the same material as the rest of the radiation shelter.

The water thickness of the radiation storm shelter depends on the amount of reserve water available. The relationship between these two variables, given a 1.5 m diameter of the spherical storm shelter, is shown in figure 15. In this thesis the water thicknesses studied ranges from 0 to 300 cm, which corresponds to between 0 and 219 thousand litres (219 tonnes).

Three days worth of consumption water is here assumed to be the minimum amount of water needed. For a crew of four astronauts, that makes 63.8 litres in total, according section 2.5.1, which equals 0.9 cm of water thickness, given the geometry of the radiation storm shelter.

[6] In order to minimize the diameter of the sphere, the upper two chairs in figure 13 are flipped forward 180°.

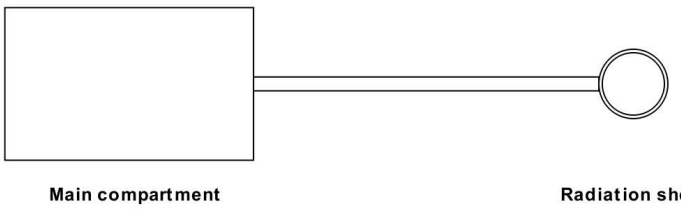

Figure 13: Schematic figure of the spacecraft divided into the main compartment and the radiation storm shelter.

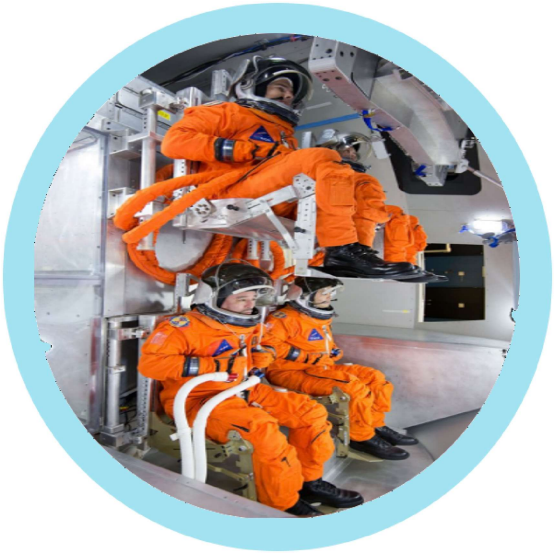

Figure 14: An approximate demonstration of the radiation storm shelter assumed in this study. The original image is taken during launch inside a mockup of the Orion spacecraft, which NASA plans on sending to Mars. Modified and reprinted from [44].

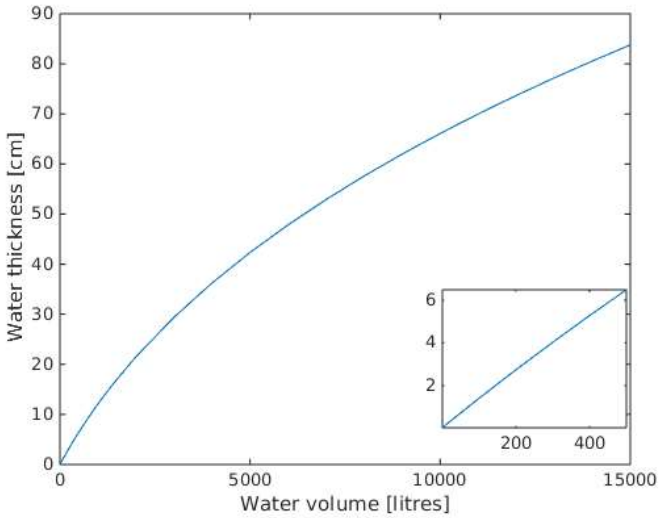

Figure 15: The thickness of the water sphere as function of the water volume available for shielding.

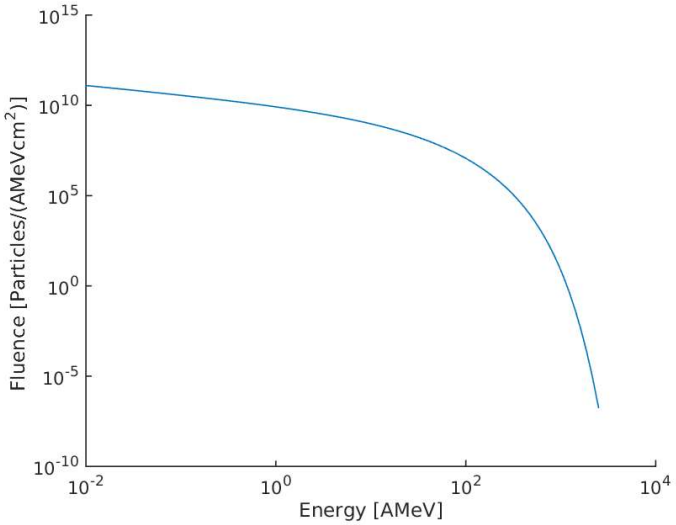

Figure 16: The differential fluence of protons from the October 1989 SPE used in OLTARIS [29]. AMeV is the particle energy, A being the particle mass number.

3.2 Dose Evaluation

The radiation dose received by an astronaut in the radiation storm shelter during a historically large SPE is modeled using OLTARIS v4.01[7] [23]. The modeling assumes only one astronaut to be inside the storm shelter, disregarding the shielding effect of the other astronauts. The historically large SPE of October 1989 was selected as a representative worst case event. Figure 16 shows the proton spectrum for this October 1989 SPE that OLTARIS uses as input.

When the SPE hits the radiation storm shelter the spacecraft is assumed to be located at 1 AU in free space. In OLTARIS the incoming stream of protons are modeled as isotropic which, according to Kouznetsov and Kundsen [10], is an acceptable approximation. Due to the isotropic radiation, the spherical structure of the storm shelter is the most effective construction to protect the astronauts from the radiation, rather than having the shielding be directional. The anatomical model placed inside the hollow water sphere is the Male Adult VoXel 2005 phantom (MAX), which is shown in figure 17.

Out of the many quantities that OLTARIS returns, the effective dose equivalent and the organ gray-equivalent (averaged to each of the body organs) were the ones studied here. The NASA quality factors and NASA tissue weighting factors for never smoker average U.S. population were selected for the effective dose equivalent calculations.

To see the influence that an additional layer of material would have on the radiation dose, a layer of a light and heavy shielding aluminum with a thickness of 5.0 and 27.5 g/cm^2, respectively, is added to the different water layers. These particular thickness values are chosen based on the shielding of the MSL/RAD where the total FOV has an average $\sim$27.5 g/cm^2 aluminum shielding and the

[7]The version refers to the version of TARIS. TARIS FORTRAN is the primary execution environment and runs on the compute cluster.

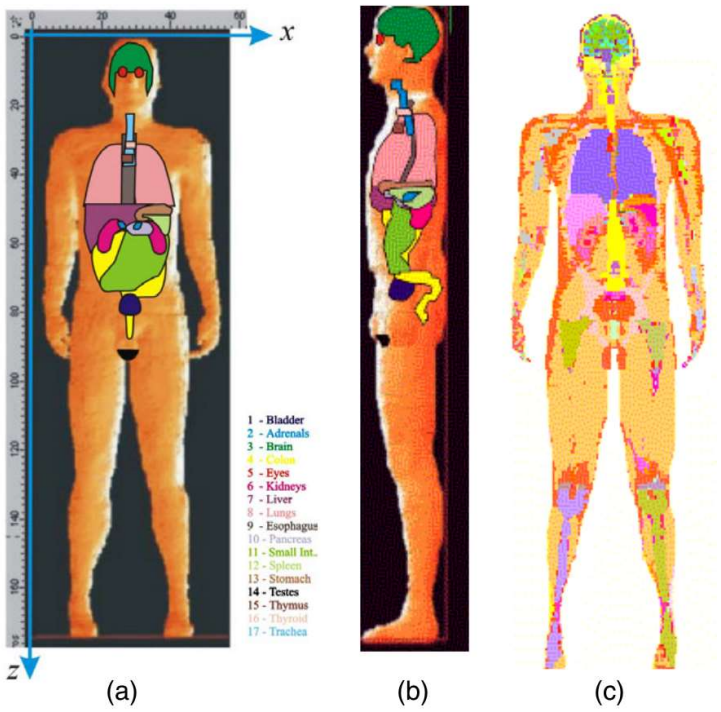

Figure 17: The Mail Adult VoXel (MAX) 2005 phantom (a) frontal view, (b) lateral view (c) centre plane cut [25]. Printed with permission.

lower part of the detector has $\sim$5 g/cm^2 average shielding [21]. A 5 g/cm^2 and 27.5 g/cm^2 Al thickness corresponds to about 1.9 and 10.2 cm of aluminum, respectively.

The study can be split in two parts: The study of the organ gray-equivalent and the study of the effective dose equivalent. Both are provided as outputs in OLTARIS. These radiological quantities can be compared directly to NASA's radiation limits for deterministic and stochastic effects.

3.2.1 Organ Dose Evaluation

NASA has defined radiation short term or non-cancer limits for the lens, skin, blood forming organs (BFO), heart and central nervous system (CNS), in units of gray-equivalent and these are the organ doses studied here. For each organ, the gray-equivalent from an SPE equal to the October 1989 event is evaluated for shielding with varying water thicknesses, in addition to 0.0, 5.0 and 27.5 g/cm^2 Al shielding. The resulting organ doses are compared to the NASA 30 day short term or non-cancer limits.

The organ dose contribution from the GCR during these 30 days is estimated by performing another analysis in OLTARIS. Assuming the same GCR spectrum properties as during the time when MSL/RAD traveled to Mars, the average GCR dose per day was found and multiplied by thirty to estimate the thirty day GCR dose contribution. The average shielding thickness, 27.5 g/cm^2, of the field of view of the RAD during transit is assumed for consistency with the GCR contribution in the effective dose equivalent evaluation below. This corresponds to the crew staying in the main compartment at all times except during the SPE when they seek protection in the radiation storm shelter. The resulting thirty day GCR dose contribution was accounted for by subtracting it from the NASA thirty day short term or non-cancer limits, for each organ.

The water thickness needed for the astronauts not to exceed NASA's limit, for each organ, is evaluated by finding the intersection of the organ dose curves and the NASA dose limits. This was done by applying a Piecewise Cubic Hermite Interpolating Polynomial (PCHP) on the data. The resulting water thicknesses needed to keep the astronauts under the organ dose limits, assuming dose contribution from SPE and GCR, are summarized. For comparison, the water thickness corresponding to the amount of water needed for 3 days for the crew of four (63.8 litres), given the 1.5 m diameter spherical storm shelter, is also shown.

3.2.2 Effective Dose Equivalent Evaluation

The study of the effective dose equivalent includes the evaluation of SPE and GCR contribution, respectively. Firstly, the radiation dose contribution from the SPE is assumed to be the only dose contribution and the results are compared to the NASA 1 year mission limit for a 3% REID (risk of exposure-induced death). The NASA 2012 values for never-smokers are used for 30 and 50 year old males and females. Secondly, a 1 year GCR dose contribution is taken into account, representing the dose contribution when travelling back and forth to Mars, where each transit takes 180 days. Here, the dose contribution from the stay on Mars is disregarded, i.e. the crew is assumed to travel continuously back and forth to Mars for a total of 360 days. The effective dose equivalent used

for the total GCR contribution is 662 mSv based on the average value from the MSL transit measurements [12].

The effective dose equivalent modelled for a spherical shield of varying water thicknesses in addition to 0.0, 5.0 and 27.5 g/cm^2 Al shielding is presented, with and without the GCR dose contribution in addition to the SPE dose. NASA's 1 year mission limits for never smoker U.S. average 30 and 50 year old female and male astronauts, are used for comparison. The estimation of the water thickness needed for the astronauts not to exceed NASA's limit is done in the same way as above, by the intersection of the effective dose curves and the NASA dose limit. The water thicknesses needed to stay under the dose limits are then presented for all astronauts with and without the GCR contribution in addition to an SPE equal to the October event. Again, for comparison, the water thickness corresponding to the amount of water needed for 3 days for the crew of four is shown.

4 Results and Discussion

4.1 Organ Dose Evaluation

Estimations of the organ doses for the lens, skin, BFO, heart and CNS, in units of gray-equivalent, are shown in figures 18, 19 and 20. The organ dose values are presented as a function of the water thickness used for shielding during the 1989 SPE with water as the only shielding material and with an addition of 5.0 or 27.5 g/cm^2 aluminum shielding. The NASA 30 day limits are presented as horizontal lines for each organ. The inclusion of the GCR contribution is represented by another line (the 30 day limit minus a 30 day GCR dose). The figure clearly shows that the GCR contribution is low for all organs.

Figure 21 summarizes the water thickness needed for the organ doses not to exceed the NASA 30 day limits for deterministic or non-cancer effects. The results presented are the estimations with and without the 30 day GCR contribution but they do not differ much. No additional water shielding is needed to stay under the limits if the radiation shelter has 27.5 g/cm^2 Al layer so 27.5 g/cm^2 Al is thus not included in figure 21.

The results with and without the 30 day GCR dose contribution do not differ much so only the results with the GCR are discussed here. When water is the only shielding material the required thickness of the radiation shelter ranges from 1.7 cm for the CNS to 7.4 cm for the BFO, making the BFO the limiting factor. To obtain a 7.4 cm thickness of water in the storm shelter, 576 litres of water would be needed. If a 5 g/cm^2 Al shield is added, the water thickness needed ranges from 0 cm for the CNS to 3.6 cm for BFO, which corresponds to 265 litres of water.

According to the results, about 27 days' worth of consumption water (576 litres) is needed for sufficient protection against short term and non-cancer effects, if only water is used for shielding against a large SPE. When 5 g/cm^2 Al thickness is added, about 12 days' worth of consumption water (265 litres) is enough. That is a feasible amount of water that might be available onboard the spacecraft. For both cases, the blood forming organs are the limiting organs. No water is needed if a shielding of 27.5 g/cm^2 aluminum (or 10.2 cm) is used.

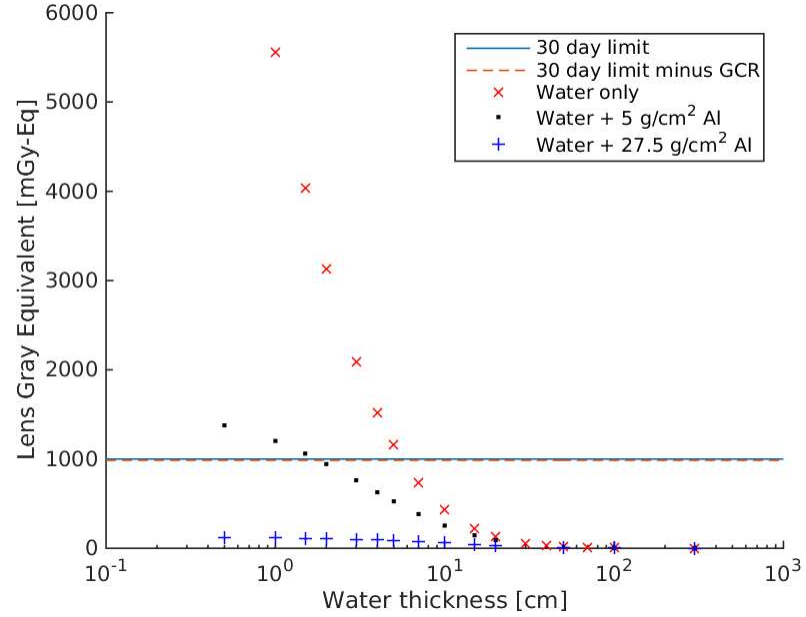

(a)

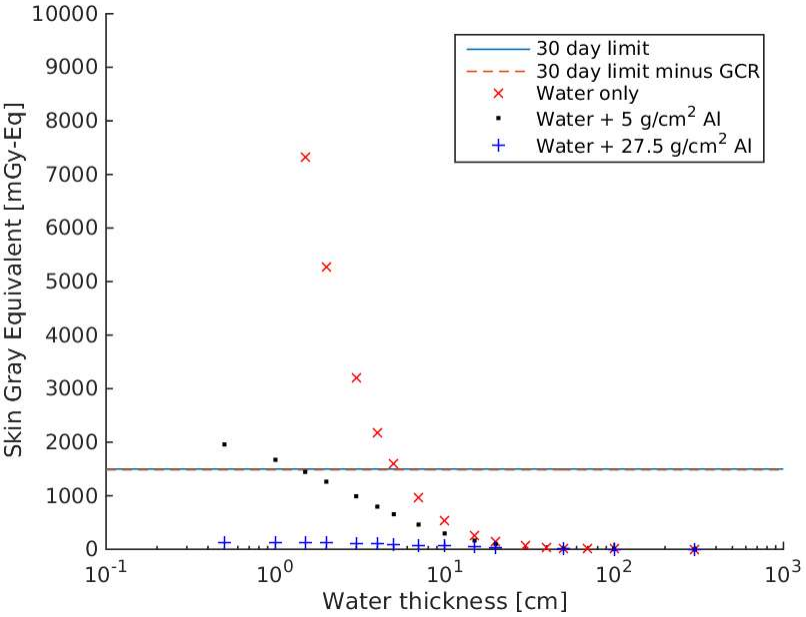

(b)

Figure 18: The gray-equivalent for (a) the lens and (b) the skin, as a function of water thickness for shielding with water only, water + 27.5 g/cm^2 Al and water + 5.0 g/cm^2 Al.

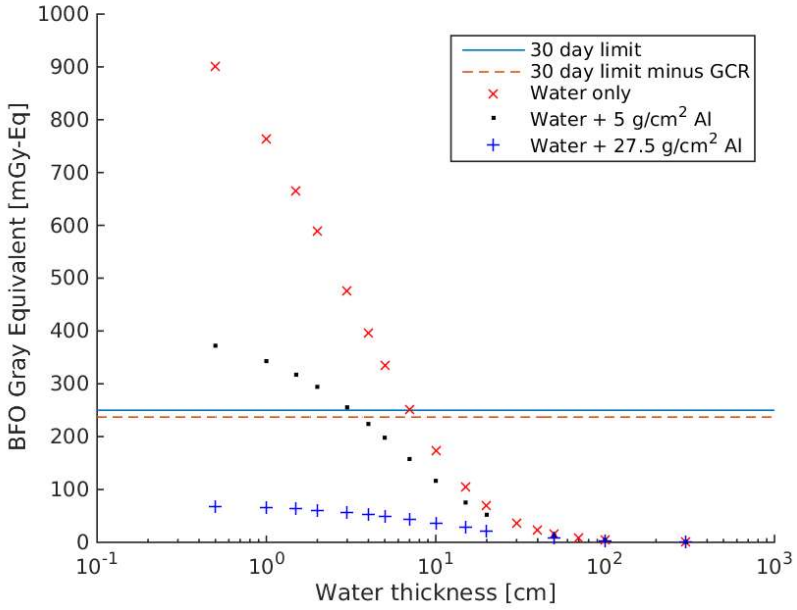

(a)

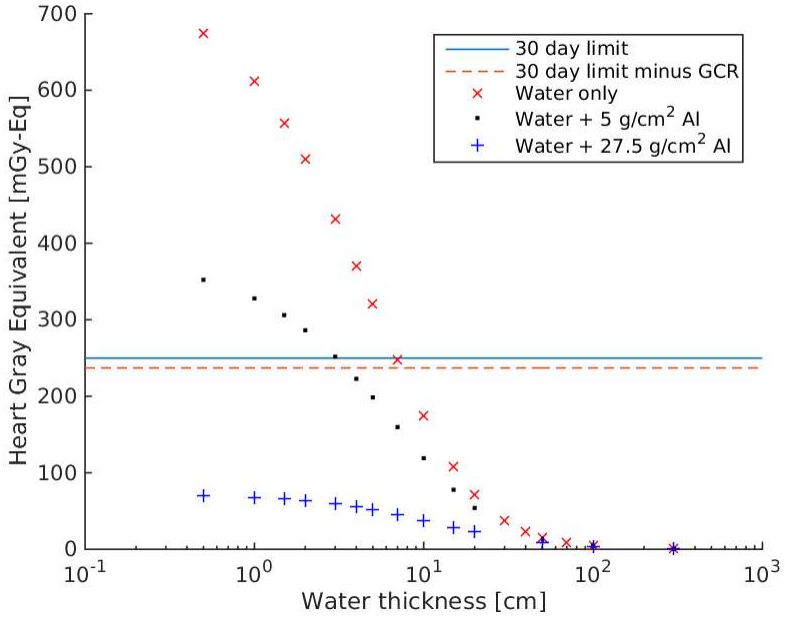

(b)

Figure 19: The gray-equivalent for (a) the BFO and (b) the heart, as a function of water thickness for shielding with water only, water + 27.5 g/cm^2 Al and water + 5 g/cm^2 Al.

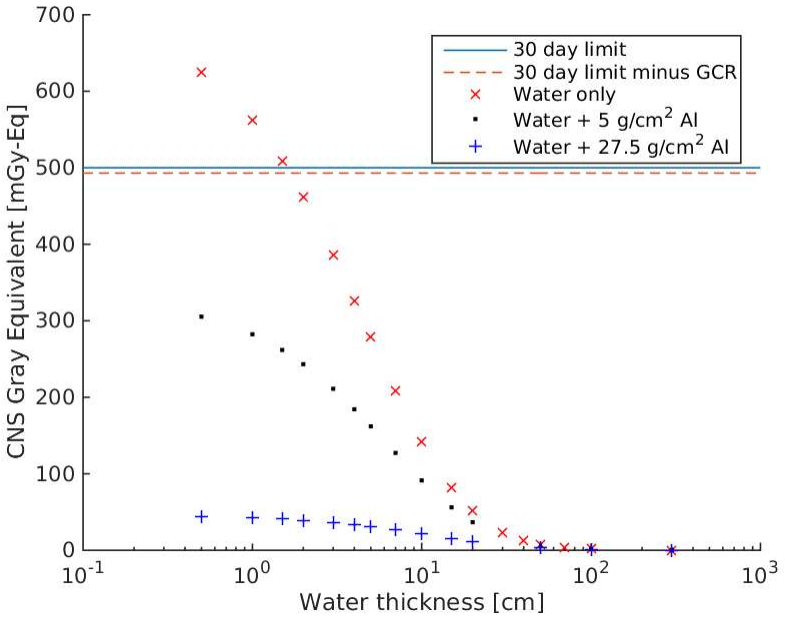

Figure 20: The gray-equivalent for the CNS as a function of water thickness for shielding with water only, water + 27.5 g/cm^2 Al and water + 5 g/cm^2 Al.

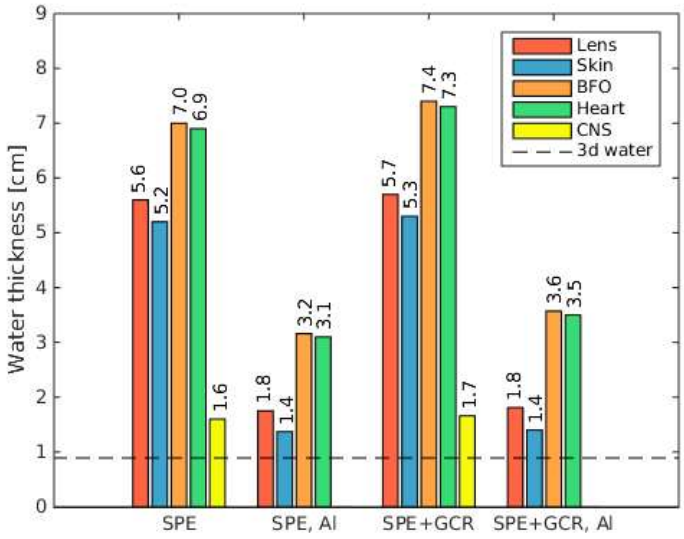

Figure 21: The thickness of water shielding needed in order not to exceed the NASA 30 day organ dose limits, assuming dose contribution from a historically large SPE and 30 days of GCR dose contribution. Shown with and without an additional 5 g/cm^2 Al shielding. A value of zero means that no water is needed. The dotted line corresponds to 3 days' worth of consumption water for the crew.

4.2 Effective Dose Equivalent Evaluation

Estimation of the effective dose equivalent, as a function of the water thickness of the radiation shelter, to an astronaut during an SPE equal to the October 1989 event is presented in figure 22. The figure shows the resulting dose when only water is used for shielding together with the addition of 5 g/cm^2 or 27.5 g/cm^2 aluminum thickness. The results are compared to the NASA 1 year dose limit for males and females of ages 30 and 50 who have never smoked [2]. In figure 22a the dose contribution is from the SPE only, i.e. the GCR dose contribution is disregarded. Figure 22b includes the effective dose equivalent contribution from the GCR inside the spacecraft's main compartment during a continuous back-and-forth transit to Mars over the course of a year.

In figure 22, the water thickness at which the interpolated effective dose equivalent values and the NASA effective dose limits intersect, corresponds to the thickness needed to stay within the NASA limits. The water thickness at the intersection points is shown in figure 23. According to the results in figure 22, a 27.5 g/cm^2 Al shield requires no water in order not to exceed the NASA limits and is thus not included in figure 23.

If only considering the dose contribution from the SPE, figure 23 shows that the water thickness needed not to exceed the NASA 1 year limit for effective dose equivalent ranges from 0 to 1.7 cm which corresponds to between 0 and 123 litres of water. With the additional 5.0 or 27.5 g/cm^2 aluminum, no extra water shielding is required.

When the GCR dose contribution is taken into account, the results are dramatically different. The GCR dose contribution from the 1 year back-and-forth journey was assumed to be 662 mSv and surpasses the 600 mSv effective dose limit for a 30 year old female without even including the SPE dose. This is represented by bars marked 'Not applicable' in figure 23 and means that a 30 year old female astronaut could not go on the journey without exceeding a 3% REID. When only water is used for shielding from the SPE, the water thickness needed for the other astronauts not to exceed the NASA limits (5.3 - 16.1 cm) corresponds to water amounts ranging from 402 and 1400 litres.

With an addition of 5 g/cm^2 of aluminum shielding, 130 to 1039 litres of water are needed to obtain the 1.8 - 12.5 cm thickness required to stay within limits. As before, a 50 year old female and 30 and 50 year old male, would need no additional water shielding if 27.5 g/cm^2 Al is included in the storm shelter.

The amount of water thus required, when solely water is used for shielding, equals between 19 and 66 days' worth of consumption water for the crew. If 5 g/cm^2 Al is added, 6 to 49 days of water supply is needed for shielding.

Comparing this with the previous findings for the organ doses, the effective dose becomes the limiting factor when both ages and genders are considered. However, if the crew were to consists of only men, older than 50, the dose to the blood forming organ would be the limiting factor.

The results demonstrate how the exposure limit dependence on the astronauts' age and sex strongly affect the amount of shielding required, which might influence who will be eligible candidates for future Mars missions.

The amount of shielding required is also strongly dependent on the GCR contribution assumed in the evaluation. If the upper limit of the MSL transit measurements of 770 mSv had been applied instead of the 662 mSv average used above, a water thickness of 8.4 - 100 cm would have been needed to not exceed

dose limits, instead of the 5.3 - 16.1 cm reported above. This example shows that there are surely many uncertainty factors that can drastically influence the results in the kind of evaluation performed here.

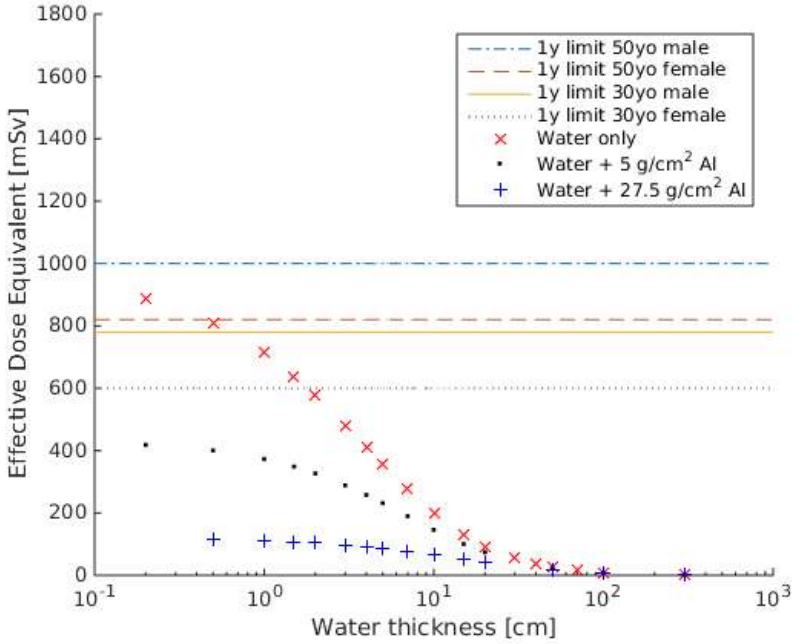

(a)

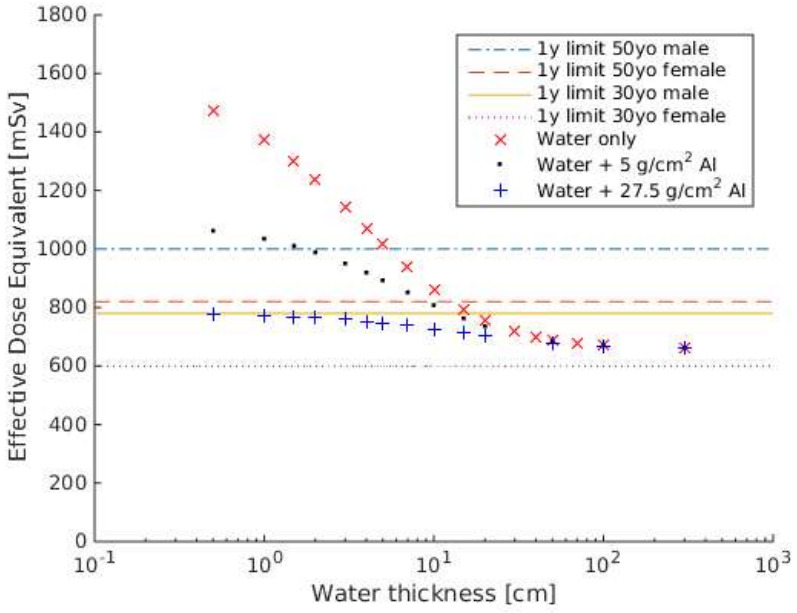

(b)

Figure 22: The effective dose equivalent for an SPE equal to the October 1989 event (a) including the dose contribution from the SPE only and (b) with the additional 1 year GCR contribution. The astronaut is assumed to be inside the spherical radiation shelter with a water wall of varying thickness and additional 0.0, 5.0 and 27.5 g/cm^2 Al shielding.

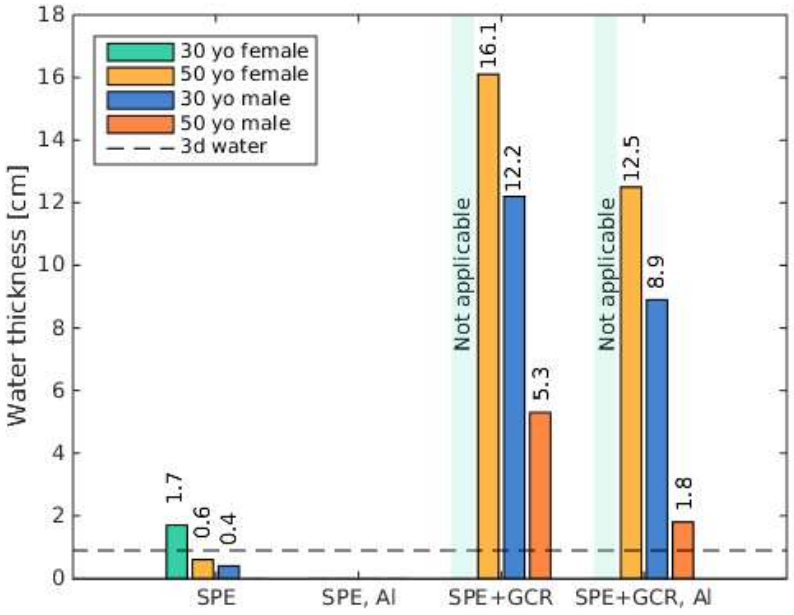

Figure 23: The thickness of water shielding needed in the storm shelter in order not to exceed the NASA 1 year effective dose equivalent limits, assuming dose contribution from a historically large SPE and GCR. Shown with and without an additional 5 g/cm^2 Al shielding. Results are presented for never smoker 30 and 50 year old female and 30 and 50 year old male. A water thickness value of zero means that the aluminum shielding attenuates the SPE-component completely (no water is needed). The dotted line is the water thickness corresponding to the amount of water needed for 3 days for the crew of four, given the storm shelter geometry.

5 Conclusions

The radiation environment in outer space poses a serious threat to humans on a mission to Mars. An acceptable risk is evaluated with respect to social and scientific benefits of the mission and with this in mind, NASA has set radiation limits that correspond to a 3% REID (risk of exposure-induced death) from cancer, in addition to limits for avoiding short term and non-cancer effects. The radiation shielding of the spacecraft is essential for the radiation exposure to be within acceptable limits and calls for cost effective and innovative shielding solutions. Hydrogen rich materials are effective for SPE shielding and one possibility is using water that will already be onboard the manned spacecraft.

In this thesis, radiation doses to astronauts were simulated with water as radiation shielding during a historically large solar particle event (SPE) in Mars transit. The focus of the simulation was on the amount of water needed to remain within the NASA dose limits when the astronauts were inside a hypothetical storm shelter. Results were obtained for SPE and GCR dose contribution for astronauts of different ages and gender, surrounded by water and aluminum of various thicknesses. The results showed that even a very thin layer of water decreases the dose to the astronauts significantly.

The most realistic scenario of those explored in this thesis, is the one where the storm shelter is surrounded by a wall of aluminum of 5 g/cm^2 thickness. This most closely resembles the real world scenario where the storm shelter is inside the main compartment of the spaceship and thereby surrounded by its outer walls. The exact thickness of these outer walls in future missions is yet to be decided but for comparison, the Apollo missions had a shielding of 4.5 g/cm^2 aluminum [45].

The results of the simulations performed show that a spherical layer of water can protect the astronauts from exceeding the NASA radiation limits during the SPE. If only the radiation exposure during the SPE is taken into account, a water layer of 3.2 cm thickness is sufficient shielding. This corresponds to 236 litres of water, equivalent to about 10 days of minimal water usage. A thinner water layer would risk radiation dose to the astronauts' blood forming organs to exceed the limits set by NASA.

During the trip, however, the astronauts are constantly exposed to the GCR, lowering the dose they can safely receive during an SPE. When taking this long-term GCR exposure into account, the simulations show that a thicker layer of water is needed to stay within the NASA radiation limits during the SPE, as is to be expected. Here, the age and gender of the crew members becomes a factor. If the crew were to include a 30 year old man[8], 8.9 cm of water would be needed to stay within 1 year effective dose equivalent limits. If all crew members were at least 50 year old men, the dose limit to the blood forming organ would again become the limiting factor, requiring a water shield of 3.6 cm. Thus, when factoring in GCR, between 265 and 707 litres of water are needed, depending on the composition of the crew. This corresponds to between 12 and 33 days of minimum water usage for the crew. These amounts are comparable to the reserve water that might be available in future Mars missions.

In conclusion, it is feasible to use consumption water as shielding during a historically large solar particle event, under the assumptions made in this

[8]The GCR contribution already exceeds the 1 year limit of 600 mSv effective dose equivalent for 30 year old women, so no amount of water shielding during SPE is sufficient.

thesis. Water is thus a promising candidate material for radiation shielding in the ongoing optimisation of a human mission to Mars.

The scope of this thesis is limited and many simplifying assumptions were made. Here, the dose from a single historically large SPE was studied but for an even more conservative dose estimate it would be preferable to include the cumulative dose over 30 days or 1 year, since more than one SPE can take place within a short time interval. Further studies could complement this work by including rigorous uncertainty estimations and a direct comparison between simulation and experimental data. Although there are still many unknowns regarding the future Mars missions, more realistic simulations can be performed as more details become available, such as the exact amount of reserve water available, geometry of the spaceship, timing and duration of the missions and ages and genders of the crew members.

References

[1] ICRP, "Assessment of radiation exposure of astronauts in space. ICRP Publication 123.," *Ann. ICRP*, vol. 42, no. 4, 2013.

[2] F. A. Cucinotta, M.-H. Y. Kim, and L. Chappell, "Space radiation cancer risk projections and uncertainties-2012. NASA TP 2013–217375; 2013."

[3] F. A. Cucinotta, S. Hu, N. A. Schwadron, K. Kozarev, L. W. Townsend, and M.-H. Y. Kim, "Space radiation risk limits and Earth-Moon-Mars environmental models," *Space Weather*, vol. 8, no. 12, 2010.

[4] "Learning Launchers: Radiation." `https://www.nasa.gov/sites/default/files/thumbnails/image/edu_stem_ll_radiation.jpg`, 2018. Accessed: 18-06-18.

[5] O. Jäkel, "Radiation hazard during a manned mission to Mars," *Zeitschrift für Medizinische Physik*, vol. 14, no. 4, pp. 267–272, 2004.

[6] F. A. Cucinotta, W. Schimmerling, J. W. Wilson, L. E. Peterson, G. D. Badhwar, P. B. Saganti, and J. F. Dicello, "Space radiation cancer risk projections for exploration missions: uncertainty reduction and mitigation," *NASA Center for Aerospace Information and NASA Langley Research Center. NASA TP-2002-210777, Scientific and Technical Information Program, Houston, TX*, 2002.

[7] M. Shea and D. Smart, "Significant proton events of solar cycle 22 and a comparison with events of previous solar cycles," *Advances in Space Research*, vol. 14, no. 10, pp. 631–638, 1994.

[8] S. Aghara, S. Sriprisan, R. Singleterry, and T. Sato, "Shielding evaluation for solar particle events using MCNPX, PHITS and OLTARIS codes," *Life sciences in space research*, vol. 4, pp. 79–91, 2015.

[9] S. El-Jaby, B. J. Lewis, and L. Tomi, "On the decision making criteria for cis-lunar reference mission scenarios," *Life Sciences in Space Research*, vol. 21, pp. 25–39, 2019.

[10] A. Kouznetsov and D. Knudsen, "Forward mapping of solar energetic proton distributions through the geomagnetic field," *Journal of Geophysical Research: Space Physics*, vol. 118, no. 8, pp. 4724–4738, 2013.

[11] J. P. Grotzinger, J. Crisp, A. R. Vasavada, R. C. Anderson, C. J. Baker, R. Barry, D. F. Blake, P. Conrad, K. S. Edgett, B. Ferdowski, *et al.*, "Mars Science Laboratory mission and science investigation," *Space science reviews*, vol. 170, no. 1-4, pp. 5–56, 2012.

[12] D. M. Hassler, C. Zeitlin, R. F. Wimmer-Schweingruber, B. Ehresmann, S. Rafkin, J. L. Eigenbrode, D. E. Brinza, G. Weigle, S. Böttcher, E. Böhm, *et al.*, "Mars' surface radiation environment measured with the Mars Science Laboratory's Curiosity rover," *Science*, vol. 343, no. 6169, p. 1244797, 2014.

[13] "Instruments. Mars Science Laboratory, Curiosity Rover." `https://mars.nasa.gov/msl/mission/instruments/`. Accessed: 2018-08-01.

[14] NASA/JPL-Caltech, "PIA14831: Mars Science Laboratory Spacecraft During Cruise, Artist's Concept.." `https://photojournal.jpl.nasa.gov/catalog/PIA14831`, 2011. Accessed: 2019-12-08.

[15] NASA, "MSL Science Corner, Radiation Assessment Detector (RAD).." `https://msl-scicorner.jpl.nasa.gov/Instruments/RAD/`. Accessed: 2019-12-08.

[16] D. Hassler, C. Zeitlin, R. Wimmer-Schweingruber, S. Böttcher, C. Martin, J. Andrews, E. Böhm, D. Brinza, M. Bullock, S. Burmeister, *et al.*, "The radiation assessment detector (RAD) investigation," *Space science reviews*, vol. 170, no. 1-4, pp. 503–558, 2012.

[17] J. Guo, C. Zeitlin, R. F. Wimmer-Schweingruber, D. M. Hassler, A. Posner, B. Heber, J. Köhler, S. Rafkin, B. Ehresmann, J. K. Appel, *et al.*, " Variations of dose rate observed by MSL/RAD in transit to Mars," *Astronomy & Astrophysics*, vol. 577, p. A58, 2015.

[18] C. Zeitlin, D. Hassler, F. Cucinotta, B. Ehresmann, R. Wimmer-Schweingruber, D. Brinza, S. Kang, G. Weigle, S. Böttcher, E. Böhm, *et al.*, "Measurements of energetic particle radiation in transit to Mars on the Mars Science Laboratory," *Science*, vol. 340, no. 6136, pp. 1080–1084, 2013.

[19] J. Guo, C. Zeitlin, R. F. Wimmer-Schweingruber, D. M. Hassler, B. Ehresmann, J. Köhler, E. Böhm, S. Böttcher, D. Brinza, S. Burmeister, *et al.*, "MSL-RAD radiation environment measurements," *Radiation protection dosimetry*, vol. 166, no. 1-4, pp. 290–294, 2015.

[20] J. Köhler, B. Ehresmann, C. Zeitlin, R. Wimmer-Schweingruber, D. Hassler, G. Reitz, D. Brinza, J. Appel, S. Böttcher, E. Böhm, *et al.*, "Measurements of the neutron spectrum in transit to Mars on the Mars Science Laboratory," *Life sciences in space research*, vol. 5, pp. 6–12, 2015.

[21] B. Ehresmann, D. M. Hassler, C. Zeitlin, J. Guo, J. Köhler, R. F. Wimmer-Schweingruber, J. K. Appel, D. E. Brinza, S. C. Rafkin, S. I. Böttcher, *et al.*, "Charged particle spectra measured during the transit to Mars with the Mars Science Laboratory Radiation Assessment Detector (MSL/RAD)," *Life Sciences in Space Research*, vol. 10, pp. 29–37, 2016.

[22] NASA, "Radiation Assessment Detector (RAD)." `https://mars.nasa.gov/msl/spacecraft/instruments/rad/`. Accessed: 2019-12-08.

[23] R. C. Singleterry, S. R. Blattnig, M. S. Clowdsley, G. D. Qualls, C. A. Sandridge, L. C. Simonsen, T. C. Slaba, S. A. Walker, F. F. Badavi, J. L. Spangler, *et al.*, "OLTARIS: On-line tool for the assessment of radiation in space," *Acta Astronautica*, vol. 68, no. 7, pp. 1086–1097, 2011.

[24] T. Slaba, G. Qualls, M. Clowdsley, S. Blattnig, S. Walker, and L. Simonsen, "Utilization of CAM, CAF, MAX, and FAX for space radiation analyses using HZETRN," *Advances in Space Research*, vol. 45, no. 7, pp. 866–883, 2010.

[25] R. Kramer, J. Vieira, H. Khoury, F. Lima, and D. Fuelle, "All about MAX: a male adult voxel phantom for Monte Carlo calculations in radiation protection dosimetry," *Physics in medicine and biology*, vol. 48, no. 10, p. 1239, 2003.

[26] J. W. Wilson, G. D. Angelis, F. A. Cucinotta, N. Yoshizawa, and F. F. Badavi, "Implementation of Gy-Eq for deterministic effects limitation in shield design," *Journal of radiation research*, vol. 43, pp. S103–106, 2002.

[27] National Council on Radiation Protection and Measurements (NCRP), "Radiation protection guidance for activities in low-Earth orbit," vol. Rep. 132, 2001.

[28] "Oltaris: Radiation uncertainties for constellation missions." `https://oltaris.larc.nasa.gov/help_documentation/uncertainties.html`. Accessed: 2018-23-07.

[29] OLTARIS, "OLTARIS: On line tool for the Assessment of Radiation in Space." `https://oltaris.larc.nasa.gov`, 2017. Accessed: 2017-03-26.

[30] ICRP, "The 2007 Recommendations of the International Commission on Radiological Protection. ICRP Publication 103.," *Ann. ICRP*, vol. 37, no. 2-4, 2007.

[31] National Council on Radiation Protection and Measurements (NCRP), "Operational Radiation Safety Program for Astronauts in Low Earth Orbit: A Basic Framework," vol. Rep. 142, 2002.

[32] F. A. Cucinotta, M.-H. Y. Kim, and L. J. Chappell, "Space radiation cancer risk projections and uncertainties-2010," 2011.

[33] R. Williams, "NASA space flight human-system standard volume 1, revision A: Crew health," 2015.

[34] M. A. Simon, J. Cerro, and M. Clowdsley, "RadWorks storm shelter design for solar particle event shielding," in *AIAA SPACE 2013 Conference and Exposition*, p. 5435, 2013.

[35] S. A. Thibeault, J. H. Kang, G. Sauti, C. Park, C. C. Fay, and G. C. King, "Nanomaterials for radiation shielding," *MRS Bulletin*, vol. 40, no. 10, pp. 836–841, 2015.

[36] F. A. Cucinotta, M.-H. Y. Kim, and L. J. Chappell, "Evaluating shielding approaches to reduce space radiation cancer risks," *NASA Technical Memorandum*, vol. 217361, 2012.

[37] G. A. Nelson, "Space radiation and human exposures, a primer," *Radiation research*, vol. 185, no. 4, pp. 349–358, 2016.

[38] S. A. Thibeault, C. C. Fay, S. E. Lowther, K. D. Earle, G. Sauti, J. H. Kang, C. Park, and A. M. McMullen, "Radiation Shielding Materials Containing Hydrogen, Boron, and Nitrogen: Systematic Computational and Experimental Study. Phase I. NIAC Final report. (NASA Innovative Advanced Concepts Program), available at `https://ntrs.nasa.gov/archive/nasa/casi.ntrs.nasa.gov/20160010096.pdf` (accessed April 2020)," 2012.

[39] H. W. Jones, J. W. Fisher, L. D. Delzeit, M. T. Flynn, and M. H. Kliss, "Developing the water supply system for travel to Mars," 2016.

[40] S. X, "Falcon Heavy space rocket." http://www.spacex.com/falcon-heavy, 2017. Accessed: 2017-05-14.

[41] NASA and K. Dismukes, "Supply and waste water." https://spaceflight.nasa.gov/shuttle/reference/shutref/orbiter/eclss/water.html, 2002. Accessed: 2017-05-19.

[42] NASA and M. Garcia, "Proposed station water system looks to retired shuttles." https://www.nasa.gov/feature/proposed-station-water-system-looks-to-retired-shuttles, 2015. Accessed: 2017-05-19.

[43] B. G. Drake, S. J. Hoffman, and D. W. Beatty, "Human exploration of mars design reference architecture 5.0," *Aerospace Conference*, 2010.

[44] "Wikimedia Commons." https://commons.wikimedia.org/w/index.php?title=File:MACES_in_Orion_mock-up.jpg&oldid=212911478, 2016. Accessed 2018-08-11.

[45] J. W. Wilson, *Galactic and solar cosmic ray shielding in deep space*, vol. 3682. NASA, Langley Research Center, 1997.